“SIMULATION OF METHANE REFORMING IN A FLUIDIZED BED REACTOR USING CFD”

A DISSERTATION

Submitted in partial fulfillment of the requirements for the award of the degree of

INTEGRATED DUAL DEGREE

(Bachelor of technology & Master of Technology)

in

CHEMCIAL ENGINEERING

(With Specialization in Hydrocarbon Engineering)

By

BHASKAR MAHATO

DEPARTMENT OF CHEMICAL ENGINEERING

INDIAN INSTITUTE OF TECHNOLOGY ROORKEE , ROORKEE-247667

CANDIDATE’S DECLARATION

I hereby declare that the work being presented in the dissertation titled **"Simulation of methane reforming in fluidized bed reactor"** is submitted in partial fulfillment of the requirements for the award of of Integrated Dual Degree. (Bachelor of Technology and Master of Technology) in Chemical Engineering (Specialization in Hydrocarbon Engineering) submitted in the Department of Chemical Engineering of the Indian Institute of Technology, Roorkee, is an authentic record of my work carried out during the period from May 2013 to June 2014 under the supervision of Dr.V.K.Agarwal , Professor, Department of Chemical Engineering, Indian Institute of Technology Roorkee, India.

The matter presented in this report has not been submitted by me for the award of any other degree of this or at any other institute.

Place Bhaskar Mahato

Date: Enrolment No. 09118024

CERTIFICATE

This is to certify that the above statement made by the candidate is correct to the best of my knowledge and belief.

Dr. V.K.Agarwal
Professor
Department of Chemical Engineering
Indian Institute of Technology Roorkee,
Roorkee,Uttrakhand-247667

ACKNOWLEDGEMENT

`

I owe a great many thanks to all those who were of immense help and supported me during writing of this dissertation. I wish to express my sincere gratitude to **Dr. V.K.Agarwal**, Professor and HOD, Department of Chemical Engineering, Indian Institute of Technology Roorkee, for providing me an opportunity to work under his guidance. His superb guidance with enriched knowledge, regular encouragement and invaluable suggestions at every stage of the present work has proved to be extremely beneficial to me. Also I would like to thank and express my gratitude to Mr. Umesh kumar, PhD scholar Chemical Engineering, Indian Institute of Technology Roorkee, for guiding and correcting various documents of mine with attention and care and helping me during different problems encountered in course of my work. I also wish to express my gratitude to my parents for their love, faith and support.

Date: Bhaskar Mahato

Place:

ABSTRACT

A two dimensional (2D) transient simulation is carried out to simulate oxidative reforming of methane in a fluidized bed reactor for hydrogen production using the computational fluid dynamics software FLUENT 14.5. The two fluid approach along with equations for species transport is used to model the reactor. Combustion, steam reforming, dry reforming and shift reactions are incorporated in the reaction model and laminar finite rate model available in Fluent is used to model the reactions. Gidaspow drag model is used to model the interactions occurring between gas and solid phase in the reactor.

The results have been validated again simulations done previously. The results show that model can satisfactorily represent the reforming of methane in a fluidized bed reactor. Hydrodynamics of the fluidized bed is also studied. The product gases mainly consists of Syngas and unreacted gases. The effect of carbon dioxide addition to the feed on hydrogen production has been studied and it was found to increase the hydrogen production. Increase in the feed temperature was found to increase the hydrogen production by it also increases the operating costs. Problem of hot spot formation was also found within the reactor. As the space velocity was increased the methane conversion and hydrogen production were found to decrease. Increasing the content of oxygen in the feed increased the conversion of methane . It was found to increase the hydrogen production and then reduce it after a certain ratio.

CONTENTS

Table of Figures

LIST OF TABLES

NOMENCLATURE

ρ_s Density of Phase k=g(gas), s(solid)

ε_s	Volume fraction of phase k=g(gas), s(solid)
υ_s	Velocity of phase k=g(gas),s(solid)
μ_g	Gas phase laminar viscosity
P_s	Pressure
d_p	Particle diameter
t	Time(s)
u	Velocity component in radial direction
v	Velocity component in axial direction
θ_s	Solid phase granular temperature(m2/s2)
τ_s	Viscous stress tensors(Pa)
K_s	Diffusion coefficient of granular temperature
Re	Particle Reynolds number
L	Axial Height (m)
C_D	Drag coefficient
e_{ss}	Coefficient of restitution between particles of solid phase
g	Vector representation of acceleration due to gravity
g_o	Radial distribution function between particles belonging to solid phase,s
K_{sg}	Momentum exchange coefficient between phase s and phase g
Υ_s	Collision dissipation of granular temperature

CHAPTER 1

1. INTRODUCTION

The world's consumption of energy is predicted to rise rapidly due to the advances in the living standards of people in developing economies and development and increased industrialization of the global economy. Petroleum based fuels rose to the forefront and became the primary source of energy for transportation needs in the 20th century and this trend has continued in the 21st century. The increasing consumption of fossil fuels such as gasoline, diesel and natural gas to meet the worlds energy requirements has increased the concentrations of carbon dioxide in the atmosphere and created problem of global warming. Petroleum is exhaustible resource and is geographically concentrated. To increase the sustainability of the energy consideration has to be given to avoid spoilage of natural resources whose availability will be crucial for the coming generations. One possibility is to enhance availability of fossil based fuels without CO_2 emissions by developing technologies for hydrogen production mainly from methane.

1.1 Hydrogen and Syngas

Hydrogen is being increasingly considered as an important alternative energy carrier for sustainable energy in the future. Hydrogen is not a primary source of energy, i.e. it does not occur naturally . It is secondary and has to be derived from other sources like electricity, fossil fuels.

Technologies using hydrogen for energy production can provide sustainable options for fulfilling the world's energy requirement. Hydrogen can play an important role in all the sectors which are major consumers of energy including -building, transportation, utilities and industry. It will also provide a means to store energy generated from renewable resources such as hydroelectric, photo-voltaic , wind and geothermal energy. Hydrogen is a clean fuel with no CO_2 emissions and hydrogen has energy content of 122 MJ/kg which is 2.75 the times of the energy content of a hydrocarbon fuel.

But there are several economic and technological barriers . This is primarily because hydrogen is gaseous at normal temperature and pressure, which must be overcome to make hydrogen competitive with the other energy sources. Advances are needed in hydrogen production system, storage, transportation , utilization and integration of these technologies with the existing ones. Biomass has great potential but still more than half of the hydrogen produced is obtained from thermo-catalytic and gasification processes which use natural gas as the main feed stock. Heavy

oil and naphtha constitute next big source for raw material. So improvement in these technologies which use fossil fuels will also be vital for sustainable hydrogen economy in the future. Different methods being explored for storage of hydrogen include metal hydrides, carbon nanotubes, alanates, borohydrides, methane methanol, light hydrocarbon.

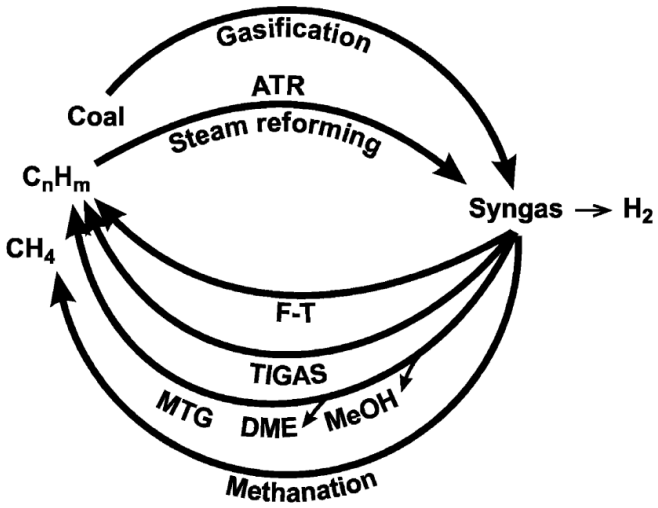

Fig1.1 The syngas cycle

Syngas is a mixture of hydrogen and carbon mono-oxide in varying ratios. The H_2/CO ratio determines the usability of the and properties of the syngas available. The various chemical and physical properties depend on this ratio. The optimum value for FT process is less than 3.5. This ratio can controlled by controlling the temperature, pressure, steam content in the reforming reactions.

The name Syngas comes from its use to create synthetic fuels, methanol and ammonia. Syngas has lesser energy density than natural gas. It is combustible and can be used in the internal combustion engines and as intermediate for other chemicals.

Most of the syngas is produced by reforming of methane. It is also important because of its availability. Coal is also an attractive option but has higher capital cost. Since methane is in gaseous form it has higher transportation and storage cost as compared to liquid and solids which increases the production cost. Thus it is a case of higher capital cost vs. higher operating cost and economic analysis can decide which feed to use.

Methane which is main feedstock in reforming processes is important for the manufacture of important chemicals and GTL technologies. The major GTL technology which is being used is the Fischer-Tropsch process. Methane is converted to syngas by reforming process and syngas is used to produce a variety of different liquid hydrocarbons.

Another method converts syngas to methanol by Cu/ZnO catalyst and then using ZSM-5, a zeolite catalyst.

Syngas is also used for the manufacture of some important chemicals. Ammonia is the largest consumer of syngas. Another chemical which uses ammonia is methanol. Combined use of natural gas for producing these two chemicals exceeded 100 billion NM^3.

The main uses are

1. Urea production
2. Blending of gasoline with chemicals produced by syngas
3. Ammonia Production
4. Methanol production

1.2 Syngas from Methane

Gas to Liquid technologies which are in focus now include FT synthesis of hydrocarbons. Syngas can be produced from a variety of feed stocks including hydrocarbons, coal, petroleum, coke and biomass, but the lowest cost methods use methane.GTL technology has focused mainly on associated gas. The main technologies which are used for producing syngas are steam methane reforming, two step reforming, auto thermal reforming, partial oxidation and heat exchange reforming. Fischer-Tropsch technology is key for all schemes of converting syngas to transportation fuels and liquid products. But syngas production itself accounts for more than 50% of the cost of a GTL plant. The technology used for the production of syngas has profoundly impacts many facets of the design of GTL plant such as plant design and location, need for oxygen and oxygen enrichment facilities, cost of downstream handling, syngas composition , gas compressors and scope and configuration of power generation alternatives.

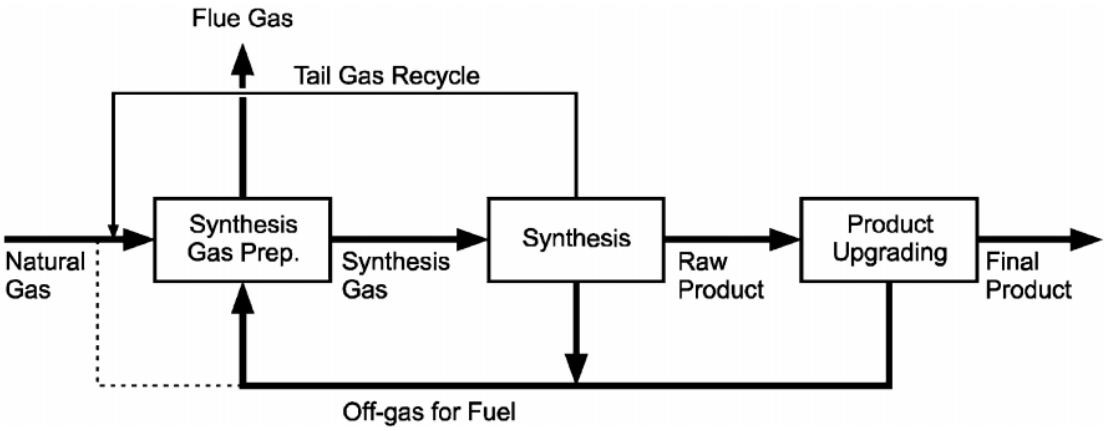

Fig 1.2 Low temperature F-T process

1.3 Technologies for reforming

A number of technologies for methane reforming have been developed depending upon the feedstock available and the composition of sysgas according to its further use. The ones which are most commonly used are described below

1.3.1 Steam Methane reforming(SMR)

Steam reforming is the oldest and most frequently used route for syngas production. As the name suggests the is process uses steam as a feed stock in conjunction with methane. Since the methane molecules are very stable severe pressure and temperature conditions are required to convert them to syngas.

Table 1.1 Different reactions in steam reforming

Reaction Name	Reaction	ΔH^0_{298k}
Steam Reforming Reaction	$CH_4 + H_20 \longleftrightarrow CO + 3H_2$	206.2 kJ/mol
Water gas Shift Reaction	$CO + H_2 \longleftrightarrow CO_2 + H_2$	-41.1 kJ/mol

Overall process is endothermic and in accordance with Le Chatteliers principle high temperature increases the yield. The catalyst generally used is Ni based Al_2O_3. Heat utility is required to supply energy . No equipment is required for separating oxygen which reduces some of the cost. The cost is also reduced due to savings on material of construction, insulation etc because the

process operates at a lower temperature as compared to the other reforming processes . The H_2/CO ratio is higher due to use of steam as a feed stock and is higher than the ratio required for the FT process, but the high H_2/CO ratio makes it suitable for hydrogen production.

1.3.2 Dry reforming of Methane(DRM)

Dry reforming of methane uses carbon dioxide in place of steam. The water in steam reforming is replaced by CO_2. Dry reforming uses CO_2 which is a green house gas to produce hydrogen and so it is has received a lot of attention. However it produces syngas with low H_2/CO ratio which makes it suitable for GTL processes.

$$CH_4 + CO_2 \longleftrightarrow 2CO + 2\ H_2$$

Dry reforming does not use oxygen or steam. However the technology for this process is limited. It holds tremendous potential for mitigating environmental concerns because it uses two green house gases to make high energy content fuel.

1.3.3 Oxidative reforming

When oxygen is used with methane for reforming it is called oxidative reforming. The oxygen used for the process is obtained by the liquefaction of oxygen from air. The liquefaction makes the process cost intensive. But using pure oxygen increases the selectivity and hydrogen production also it avoids heat losses to inert gases like nitrogen . The main drawback is the large cost of the liquefaction plant and the operating costs for cooling and liquefaction.

1.3.4 Partial Oxidation of Methane(POX)

Partial oxidation can occur through two routes i) non catalytic partial oxidation does not use any catalyst ii) catalytic partial oxidation uses a catalyst which makes the reaction favorable and faster.

$$CH_4 + 0.5\ O_2 \longleftrightarrow CO + 2\ H_2$$

Some of the methane undergoes total oxidation to produce steam. In the presence of water steam reforming also occurs. But the process gives only moderate selectivity and a high outlet

temperature for the gases. This process gives H_2/CO ratio of about 2 which can be used for FT process . But the oxygen plant adds to the cost. But the cost of heat utility is eliminated as the energy required is obtained from the combustion reaction. By installing insulation to avoid heat losses the POX process can be achieved without any external heating.

1.3.5 Auto-thermal Reforming of Methane

As the name suggests no control is required for the temperature in case of autothermal reforming. This is because the heat of combustion of the methane compensates for the heat of the reforming reactions. The overall enthalpy of the process is made zero by adjusting the methane and oxygen ratio. The H_2/CO ratio is favourable for for FT process. The outlet temperature is also lower in autothermal reforming as compared to other reforming reactions. The need of external energy is also reduced due to the supply of energy required for the reaction by combustion. However only a few catalysts have been developed for this process. Additional plant for liquefaction of oxygen adds to the cost.

Table 1.2 List of the different reforming technologies

Technology	Advantages	Disadvantages
Steam Methane Reforming	• Widely used in the industry • Pure oxygen is not required • Lower temperature compared to other reforming reactions • Ideal for Hydrogen production	• H_2/CO is high and is not suitable for purposes where CO is also required. • Emissions into atmosphere is high.
Heat exchange reforming	• Small and compact size. • Capacity of the plant can be increased according to requirement.	• Very few commercial plants are constructed. • Has to be combined with some other syngas production process.
Two-step reforming	• Reduced plant size • Highly pure syngas is obtained • Syngas methane content can be tailored by changing secondary reformer outlet temperature	• Increased process complexity • Very few commercial plants are constructed. • Pure oxygen is required.
ATR	• H2/Co ratio suitable for GTl processes. • Lower temperature and low methane	• Limited commercial utilization. • Oxygen is required.

	slip •	
POX	• Not affected by presence of sulphur • No carbon formation occurs and no steam is needed. • H_2/CO ratio lower than 2.0 is obtained	• Not suitable for high H_2/CO requirement. • Outlet temp. is high • Oxygen is required. • Composition cannot be altered easily

1.4 Fluidized bed reactor

Fluidized bed reactor are employed in the process industry to carry out a number of multiphase chemical reactions. In this reactor a liquid or gas is passed through a granular solid material at velocities high enough to cause it behave as if it were a fluid. Advantages and disadvantages of these reactors are listed below.

Advantages

1. These reactors provide intimate contacting between the gas and solids and also provide excellent particle mixing.
2. High heat transfer gives more uniform temperature distribution and mass transfer capabilities is enhanced due to mixing

Disadvantages

1. Bypassing of the gases may occur if the distribution is not good.
2. Attrition occurs due to collision of the catalyst particles, the fines which are formed are lost from the reactor.

The most commonly used reactors are bubbling fluidized bed and circulating fluidized bed reactors.

1.5 MOTIVATION

Hydrogen and production of syngas to for production of liquid hydrocarbons to meet the increased energy needs of the world will become increasingly important in the future. Methane due to its availability will be very important in this regard. Though there has been a lot of research on the methods of steam reforming the other processes are relatively less studied. The integration of oxidation with steam reforming and carbon dioxide reforming can open up new avenues for controlling these reforming processes. Also fluidized bed reactors present a number of advantages over the conventional fixed bed reactors. So my study of reforming in such fluidized will improve the designing of such reactors and optimization of syngas production.

1.6 OBJECTIVES

- To study the hydrodynamics of the fluidized bed reactor.
- To study the effect carbon dioxide injection along with the feed on hydrogen production and conversion.
- To study the effect of addition of heat on the performance of the reactor by changing the inlet temperature and measurement of hydrogen production.
- To study the temperature profile along the length of the reactor and study the variation in temperature profile and hotspot temperature.
- To study the performance of the reactor in syngas production due to change in the oxygen feed.
- To study the effect of change in space velocity on the performance of the reactor.

CHAPTER 2

LITERATURE REVIEW

2.1 Review of Simulation studies

De Groote et al.(1995) carried simulation of out CPO of CH_4 in a fixed bed reactor under adiabatic conditions using mixture of methane and oxy gen and then methane and air. The reactions incorporated included combustion , steam reforming and shift reaction , the catalyst used was based on Ni. The model was one dimensional and radial mixing was assumed to be absent. The results found temperature to be within acceptable limits only when air was used or steam or CO_2 was used with the feed. The temperature surpassed acceptable limits when the reaction was carried out with reaching 1773 K which causes severe damage to the catalyst. The temperature was reduced when air was used or carbon dioxide was injected with the feed. The coke deposition was reduced when steam was introduced with the feed but it was distributed along greater length of the reactor.

Yin et al.(2007) simulated the dry reforming of CH_4 to study how reforming is affected by the formation of cluster of particles in fluidized reactors. The simulation was two dimensional and the catalyst was Rhenium based on Alumina. The flow of gas through the particle cluster was negligible when the void fraction was less than 0.90.The drag force acting on the particles was much reduced than the force experienced by a single particle due to the effect of other particles and differed at different location in the bed. The $H_2$and CO yields increase with the increase of inlet gas velocity and displayed a convex like behavior with increasing of inlet gas temperature. The increase of reactor pressure increased rate of dry reforming reaction and decreased the H_2/CO mole ratio.

Abashar et al.(2012) studied the distribution of oxygen along the length of the reactor for reforming using nickel catalyst. The temperature distribution and formation of hotspots had profound. The results revealed that CFFBR have a great potential for efficient hydrogen production. The distribution of oxygen along the reactor length greatly improved the performance of the reactor. Reaction runaway and formation of hotspot is stopped by the

distribution of oxygen while when oxygen was fed with methane hotspot formation was observed the highest hydrogen yield was found for a combination of co-feed and distribution along the length of the reactor.

Park et al.(2013) developed a reactor model for mixed reforming over Ni-based catalyst to investigate non-equilibrium behavior and reactions. The determination of kinetic parameters for the reactions was done by curve fitting to conversion of CH_4, CO_2 and H_2/CO ratio for different reaction conditions. Temperature, reactor pressure and hourly space velocity had significant effect on the CO_2 and CH_4 conversion. The advantages of the mixed reforming process are easy manipulation of H_2/CO ratio in the produced syngas, maximum utilization of CO_2 per unit CO productivity. H_2/CO ratio, syngas production and the yield of CO from CO_2 can be easily controlled in case of mixed reforming.

Li et al.(2008) used method of Gibbs free energy minimization to investigate the thermodynamics of CH4 autothermal reforming and also found out schemes for minimization of coke formation. Using higher temperature decreased the coke formation in case of dry reforming of methane while addition of steam eliminated it in case of steam reforming. O_2/CH_4 ratio of more than 0.4 and H_2O/CH_4 ratio of more than 1.2 is suitable for autothermal reforming. Temperature of above 700 ^oC is favorable for these reactions.. The optimal $CH_4/CO_2/O_2$ feed ratios 1:0.8–1.0:0.1–0.2 through the analysis of thermodynamic equilibrium in the oxidative CO_2 reforming corresponded to the reaction temperature higher than 800^0C. In case of oxidative dry reforming increasing the reactor pressure increased coke deposition and reduced the conversion of carbon dioxide and hydrogen yield.

Barrio et al.(2006) simulated reforming with steam and CPO on a noble metal catalyst(Ru/ Al_2O_3) and studied the temperature distribution along the length of the reactor. The reactor simulated was a small scale fixed bed reactor. Interfacial and interparticle mass transfer was assumed negligible in the simulations. The Ruthenium catalyst for reforming and partial oxidation had same order of activation energy and pre-exponential factors for Ni based catalyst. The temperature profile, product composition and flow rates were in good agreement with the

experimental results. The distribution of oxygen along the length of the reactor reduced the temperature of the hotspot and increased the stability of the catalyst.

2.2 Review of Thermodynamic studies

Freitas et al.(2012) did thermodynamic analysis by two methods Gibbs energy minimization and maximization of entropy to find out the equilibrium condition for oxidative reforming of methane. In reaction conditions the pressure was varied from 1-10 atm, temperature was varied from 600K to 1600K and the O_2/CH_4 ratio from 0.1 to 0.5. The reaction was favored at high temperature and low pressure.O_2/CH_4 ratio is an important parameter for control of the final product composition. The most favorable conditions found out by minimization of Gibbs free energy were found to be 1200K and low oxygen to carbon ratio under atmospheric pressure. The catalyst with anti coking properties increases the stability and reduces the H_2 production due to inhibition of methane decomposition to carbon and hydrogen. By the scheme of entropy maximization the overall reaction was found to be exothermic when the oxygen to methane ratio is more than 0.5 and endothermic when it was lesser than 0.5.

Avila-Neto et al.(2010) studied the thermodynamics of methane reforming .Effects of temperature, pressure, steam to carbon ratio, CH_4/CO_2 ratio and oxygen to carbon ratio and S/O/C on the products was investigated.. A one dimensional model was proposed to represent a fixed bed reactor with Ni based catalyst operating in steady state. The reactor modeled fixed bed and used Ni/Al_2O_3 catalyst. It was assumed to operate in steady state. They also investigated coke formation and the reaction conditions under which it is promoted. Using low H_2O/CH_4 ratio reduced the formation of coke. The best operating conditions for methane reforming were found out. Steam reforming gave the highest yield of hydrogen and almost 100% conversion . There was negligible deposition of coke on the Ni catalyst. The highest yield was 3.36 mol of H_2 at a temperature of 850 OC and H_2O/CH_4 ratio of 4.

2.3 Review of CFD studies

Dou et al.(2010) did a CFD simulation of steam reforming of methanol in a fluidized bed reactor. To simulate the interaction, of the solid and gaseous phases the Two fluid method was used and reactions were simulated by using the laminar finite rate model . There was a bed expansion of more than 200% under the fluidized condition. The fluidized conditions were

achieved in under 5s. Increasing the space velocity of the gas decreased the conversion of glycerol nd reduced the production of H_2 slightly. Glycerol conversion, H_2 production and selectivity increase with increasing the values of steam to carbon ratio (S/C) from 2:1 to 4:1, but there is no significant change in steam conversion with an increase in S/C.

Taghipour et al.(2005) studied the hydrodynamics of a gas-solid fluidized bed reactor experimentally and computationally. Computational results were obtained from commercial software Fluent were compared with the results obtained by the experimental results from fluidization of spherical glass beads of 250-300um diameter. Multifluid Eulerian model incorporating the kinetic theory of gases was applied to simulate the gas-solid flow. Momentum exchange coefficients were calculated using the Syamlal O'Brien, Gisdapow and Wen and Yu drag functions. Restitution coefficient ranging from .9 to .99 was used to characterize the solid phase kinetic energy fluctuation. experiments were conducted in a plexiglass column of 1 m height and .28 m width with 0.025 m thickness. The distributor plate was a perforated plate. Spherical glass beads of 250- mm diameter were fluidized. The hydrodynamic model conservation equations used were as follows (1) Mass Conservation equations (2) Momentum conservation equation (3)Gidaspow drag function (4)SyamlaO'brien drag Function (5)EMMS drag function. The equation used for kinetic theory of granular flow were (1)granular temperature and (2)Solid phase transport equation for granular temperature. Constitutive equations used were for (1)Stress tensor (2)Solid pressure (3) Radial distribution function (4)Solid bulk viscosity (5)Solid shear viscosity (6)Kinetic viscosity (7)Solid frictional viscosity. The overall pressure drop, bed expansion ratio and voidage were experimentally determined and compared with those predicted by the CFD simulation. It was found that the fluent software was capable of predicting the gas solid behavior of fluidized bed. A good agreement was found between the experimental and time average pressure drop, bed expansion and qualitative gas flow pattern.

Benzarti et al.(2012) did a parameter based study of the hydrodynamics of riser in a bubbling fluidized bed. The simulation used the two fluid model and kinetic theory of granular flow was used for simulation of the solid particles. Commercial CFD tool FLUENT was used for the simulation of a two dimensional model of the riser. Different drag models available for the interaction of the gas and solid phases such as the Gidaspow , Syamlal and O’Brien models were

studied comparatively . The simulation was done by solving the basic conservation equation of mass momentum and energy and kinetic theory of granular flow is used for modeling the interaction of the solid particles. The Gidaspow and Symalal model were found to exceed the experimental calculation while the EEMS model gave good results for dense phase formation and were in good agreement with the experimental increase of bed height. According to the results the EMMS model is suitable for simulation of particles below the size of 75 μm.

Rowshanzamir et al.(2012) simulated a 3D CFD model of monolith reactor for hydrogen production using auto thermal reforming reactions. The catalyst chosen was 5% Ru/Û-Al_2O_3. Ru catalyst is favors hydrogen production for low temperature catalytic partial oxidation (LTCPO) process and it gives high catalyst activity and high hydrogen yield. The catalyst was highly stable in the time for which the experiment was carried out. Hydrogen production was increased by the use of higher oxygen to methane and higher steam to methane ratio. The CFD results showed that Ruthenium is highly selective to hydrogen production and gives high H_2/CO syngas which is can be used for fuel cells applications by using high steam to methane ratio .

2.4 Review of Kinetics studies

Hou et al.(2000) carried out studies on the kinetics of the methane steam reforming, accompanied by the reverse water gas shift reaction over a commercial Ni/α-Al_2O_3 catalyst in an integral reactor under conditions of no diffusion limitation. . Under low methane conversion and low temperature, the rate of reaction of methane with steam was found to be first-order with regard to methane, which is suggested by methane conversion being proportional to the contact time and the partial pressure of methane. The rate of steam reforming was found to follow first order kinetics with respect to methane at low temperature. The at low conversions the rate of reaction was proportional to the methane partial pressure and the conversion was found proportional to the residence time. Temperature was a important parameter for the product composition but the effect of pressure was not evident. Hydrogen production is favored at low temperature and high SCR. Total combustion dominates the reforming reaction at low temperature there by there is faster formation of carbon dioxide as compared to carbon monoxide. The kinetic parameters estimated, gave results which were in good agreement with the experimental observations on simulation

2.5 Review of Experimental studies

Moreno et al.(2013) studied the oxidative steam reforming of CH4 in a two-zone fluidized-bed reactor (TZFBR) over a Ni/Al_2O_3 catalyst. The parameters studied were temperature SCR, OCR and GHSV.

Increasing the ratio reduced the combustion reaction and reduced the energy available for reforming thereby decreasing the methane conversion. There was also a considerable increase in the hydrogen and carbon monoxide selectivities.

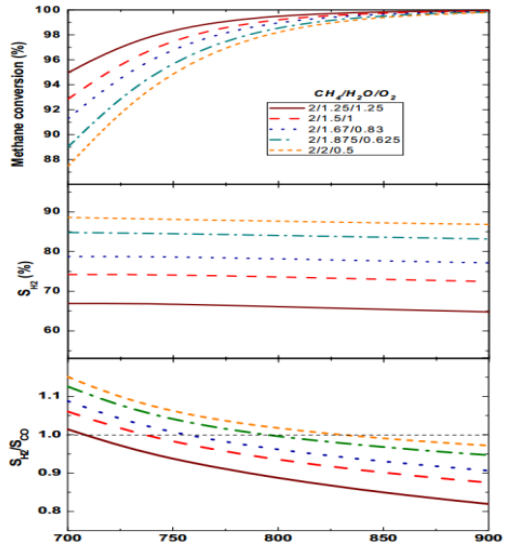

Fig 2.1 Methane conversion and CO and H2selectivities in thermodynamic equilibrium for several $CH_4/H_2O/O_2$ ratios as a function of temperature.

Corbo et al.(2006) studied the partial oxidation using different metal based catalyst. The metals used were Ni, Pt. The nickel catalyst used were based on two kind of alumina and the platinum catalyst was based on Ceria. Effects of temperature, space velocity and air/fuel molar on ratio product composition and coke formation were studied. All the catalysts were suitable for the reforming reactions only at temperatures above 973K. The carbon deposition increased with decreasing the space velocity but the activity of catalyst decreases with decreasing the residence time. The Pt catalyst had the lowest auto ignition temperature among the three catalysts. The platinum catalyst gave low selectivity and yield as compared to the Ni catalyst. The results

showed possibility of developing synergic effect between catalytic properties of Pt and Ni and possibility of exploiting $Ce0_2$ as a support due to its oxy-carrier abilities. Ceria catalyst was found to be useful due to its oxygen carrier ability and there is possibility of developing bi metallic catalyst.

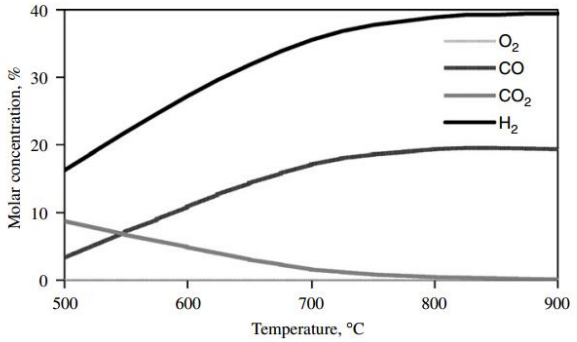

Fig 2.2 Equilibrium concentrations in the reaction products in methane CPO,O_2/C=0.50 in air/methane feed.

Jing et al.(2004) investigated the reforming of methane with CO_2 and oxygen to produce low H_2/CO ratio syngas over Ni/MgO/SiO_2 catalyst. They studied the effects of reaction temperature, space velocity and feed gas composition. The effect of fluidization on conversion of methane was also investigated. It was found that as the O_2/CO_2 ratio was increased CH_4 conversion increased due to combustion and reforming with CO_2 and O_2 and the apparent CO_2 conversion decreased due to the formation of CO2 in combustion. Also the methane conversion was found to increase with increase of temperature at constant feed composition and the conversion reached almost 87% at 1023K. As the space velocity was increased the methane conversion and H_2/CO ratio was found to decrease due to reduced contact times Because combustion is a fast process but reforming cannot reach equilibrium so fast.

Qianshan Jing et al.(2005) investigated the reforming of methane with CO_2 and oxygen with Ni/Mgo-SiO_2 catalysts. From the study it was found that methane and O_2 reforming can be performed at short contact times and nearly uniform temperature in the catalyst bed and the performance was strongly dependent on the oxidation state of the active component Ni. Oxidized

Nickel showed lower reforming activity compared to reduced Ni. The conversion almost of thermodynamic equilibrium was obtained with reduced catalyst but fresh unreduced catalyst gave higher lower conversion. There was a lot of whisker carbon formation in the rear end of the fixed bed reactor therefore the CH_4 and CO_2 conversions were lower. Two kinds of catalyst particles were found to exist one without any carbon whisker and the second with carbon whisker. The advantage of fluidized bed reactor is lower carbon deposition as compared to the fixed bed. Enhancement of the conversion occurs due to the fluidization of the catalyst in the fluidized bed reactor.

Dantas et al.(2012) studied ORM on Ni catalyst based on Al_2O_3,CeO_2/Al_2O_3 and $Ce_{0.5}Zr_{0.5}O_2$ /Al_2O_3. Kinetics parameters were taken from previous studies and the results were compared with the results from experimental results. The Ni was found to have greater dispersion and the high surface area for metal deposition. From XRD investigation it was found that there was formation of solid solution $Ce_{0.5}Zr_{0.5}O_2$ but there was no formation solid solution in case of the Alumina support. Cerium support was found to have good oxygen storage ability. Samples supported on alumina showed similar methane conversions which can be explained by similar Ni deposition. These samples showed good stability and H_2/CO ratio close to the theoretical value. Although the theoretical calculations were lower than those obtained experimentally the model was able to predict the general behavior of the system for oxidative reforming .

Zhai et al.(2010) investigated the following Ni-based catalysts namely $Ni/Zr0_2/Al_2O_3$, Ni/La-Ca/Al_2O_3 and $Ni_{0.5}Mg_{2.5}AlO_2$ for high temperature methane steam reforming at high space velocities. $Ni/ZrO_2/Al_2O_3$ and Ni/La-Ca/Al_2O_3 catalysts are poor in performance while $Ni_{0.5}Mg_{2.5}AlO_2$ exhibited good stability and activity in steam reforming at the short residence time of 20 ms and at the same time it was found to satisfy requirements of high space velocity as well. In such short contact time process, Carbon dioxide selectivity was found to have a opposite trend to CH_4 conversion. The H_2 yield depends on these two inconsistent factors. To obtain the maximum H_2 selectivity both these factors have to be taken into account and studied comprehensibly.

CHAPTER 3

CFD MODELING OF FLUIDIZED BED REACTOR

Fluidized bed reactors find application in various chemical, petrochemical and metallurgical industries, where they are used primarily to carry out gas-solid reactions . Two major application of fluidized bed are in the Fluid Catalytic Cracking and biomass gasification in the combustor section. Particle size and hydrodynamics have profound impact on the efficiency of such particles as it affects the gas solid contacting and transport of reactants and products inside the reactor. Computational Fluid Dynamics can play a major role in simulation and study of such reactors.

3.1 Gas Solid Fluidization Modeling

There are two ways to modeling of gas-solid systems in fluidized beds and it depends on the way in which the solid phase is modeled. The first approach is called the Eulerian -Eulerian approach or two fluid model where both the phases are modeled as continuous interpenetrating media. The second approach is called the Eulerian Lagrangian approach or discrete element method, where each solid particle is modeled separately as a discrete particle and only the gas phase is considered as a continuous media.

Eulerian Lagrangian model is more detailed and solid particle is studied at the particle level. In this approach the particles are considered as point masses and the discretization of the gas phase

is carried out unaffected by the solid phase as the particles are very small. The particle equation of motion can be integrated to find the path of the particle by determining the various forces such as gravity, buoyancy, drag forces on the particle.

Eulerian -Eulerian approach considers the primary and the secondary phases to be continuous . The TFM considers the solid phase as a continuous medium despite it being a discrete phase so additional laws known as closure laws are needed to describe the flow properties and rhelogy of the solid phase. The Eulerian method is less accurate but it has several advantages over the Lagrangian method which is why it is widely used in the simulation of gas-solid modeling.

- The Eulerian approach requires lesser computational effort than the Lagrangian approach.
- Addition of more particles does not cause the computational requirements to increase greatly but it increases significantly even with the addition of few more particles in the Lagrangian model.

3.2Computational Flow models

The TFM model is used here to simulate the reforming reactions of methane on Alumina based Ni catalyst using laminar finite approach for the reactions. The properties and interaction of the solid catalyst particles are determined by using kinetic theory of granular flow which assumes the solid particles to behave similarly to gas particles. The simulation is carried using academic version of ANSYS 14.5 software.

3.2.1 Solid-Gas Flow Equations

The dynamics and trajectory of each phase is calculated with the use of continuity equation for each phase.

The Continuity equation for the phase q is given by :

$$\frac{\partial}{\partial t}(\varepsilon_q \rho_q)+\nabla.(\varepsilon_q \rho_q \upsilon_q)=0 \quad (3.1)$$

q=g denotes the gas phase and q=s denotes the solid phase, velocity vector is given by υ and ρ is the density , ε is the volume fraction of the phases with the constraint.

$$\Sigma\varepsilon_q=1 \quad (3.2)$$

Momentum Equations

The momentum conservation for the gas phase is given by the following two equation:

$$\frac{\partial}{\partial t}(\varepsilon_g \rho_g)+\nabla.(\varepsilon_g \rho_g \upsilon_g)(\rho_g \varepsilon_g \upsilon_g)+\nabla.(\rho_g \varepsilon_g \upsilon_g \upsilon_g)=-\varepsilon_g \nabla P+\nabla\tau_g-K_{gs}(\upsilon_g-\upsilon_s)+\rho_g \varepsilon_g g=0 \quad (3.3)$$

$$\tau_g = \varepsilon_g \mu_g (\nabla \upsilon_g+\nabla \upsilon^T{}_g) \quad (3.4)$$

The momentum conversation for the solid phase is given by the following two equations :

$$\frac{\partial}{\partial t}(\rho_s \varepsilon_s \upsilon_s)+\nabla.(\rho_s \upsilon_s \varepsilon_s \upsilon_s) = - \varepsilon_s \nabla P + \nabla P_s + \nabla\tau_s - K_{gs} (\upsilon_s-\upsilon_g) + \rho_s \varepsilon_s g \quad (3.5)$$

$$\tau_s = 2\ \varepsilon_s \mu_s (\nabla \upsilon_s + \nabla \upsilon_s t) + \varepsilon_s (\lambda_s - \frac{2}{3}\mu_s) \nabla \upsilon_s \bar{I} \quad (3.6)$$

Properties Model Equations

The factors which determine gas and solid interaction are described by various property models for their calculation. The ones which are used are mentioned below

Granular Viscosity

The granular viscosity for the solid phase is given by the sum of the three kind of viscosities which are explained below

$$M = \mu_{s,coll} + \mu_{s,kin} + \mu_{s,fr} \quad (3.7)$$

Collisional viscosity arises due to the collision between the particles in the solid phase and it is assumed it is similar to viscosity of gases. This viscosity is defined from the kinetic theory of granular flow. The correlation given by Lun et al is as follows

$$\mu_{s,coll}= \frac{4}{3} \varepsilon_s \rho_s d_s (1+e) g_0 (\frac{\Theta_s}{\pi})^{0.5} \quad (3.8)$$

where g_θ denotes the radial distribution function, e denotes the restitution coefficient and Θ_s is the granular temperature.

$\mu_{s,kin}$ is the kinetic viscosity .Here for defining the kinetic viscosity we use the correlation given by Gidaspow.

$$\mu_{s,kin} = \frac{(10 \rho_s d_s \sqrt{\theta_s \pi}))}{96 \alpha_s (1+e_{ss}) g_{0,ss}} *[1+\frac{4}{5} g_{o,ss} \alpha_s (1+e_{ss})]^2 \quad (3.9)$$

Frictional viscosity arises due to the frictional force between the particles and it contributes to the total shear viscosity. Frictional viscosity becomes more important when the packing is greater and interaction between the particles is mainly due to rubbing. Schaefer expression for the fractional viscosity is given the following expression

$$\mu_{s,fr}=\frac{(P_{s,fr} \sin\phi)}{2 \sqrt{I_{2D}}} \quad (3.10)$$

$P_{s,fr}$ =frictional pressure , ϕ=angle of internal friction, I_{2D} = second invariant of stress tensor

Granular Bulk Viscosity

The resistance offered to compressive and expansive forces by the particles is called bulk viscosity . Lun et al developed the following formula for granular bulk viscosity

$$\lambda_s = \frac{4}{3} \varepsilon_s \rho_s d_s (1+e) g_0 (\frac{\Theta_s}{\pi})^{0.5} \quad (3.11)$$

Granular Conductivity

Granular conductivity helps determine the transfer of granular energy between the particles. It is similar to the thermal conductivity of gases and gives the diffusive flux of granular energy

$$k_s = \frac{(150*\rho_s*d_s*\sqrt{\theta_s*\pi})}{(1+\varepsilon_{ss})*g_{0,ss}} [1+\frac{6}{5}\alpha_s\, g_{0,ss}\, (1+e_{ss})]^2 + 2\varepsilon_s\ \rho_s\ g_o\ (1+e)\ (\frac{\theta_s}{\pi})^{0.5} \quad (3.12)$$

Solids pressure

The solid pressure has two parts i) collision ii) kinetic . Before the bed becomes fluidized the solid pressure is the highest. After the fluidization begins the solid pressure decreases but it again rises as the frequency of collisions increase

Lun et al gave the expression for solids pressure :

$$P_s=\rho_s\ \varepsilon_s\ \theta_s\ [1+2\ (1+e)\ \varepsilon_s\ g_0] \quad (3.13)$$

Where e = restitution coefficient.

Radial distribution function

Radial distribution function (g_0) depends on the distance between the particles and accounts for the possibility of collision between the solid particles.

$$g_0 = \frac{s+ d_p}{s} \quad (3.14)$$

where s = distance between the spheres. The above expression shows that as s approaches to infinity then the probability tends to zero and increases as the particles come closer.

$$g_0 = \frac{3}{5}\left[1 - \left(\frac{\varepsilon_s}{\varepsilon_{s,max}}\right)^{0.33}\right]^{-1} \quad (3.15)$$

$\varepsilon_{s,max}$ is the particle volume fraction at maximum packing.

Granular Temperature

The kinetic energy contained by the solid particles due to their arbitrary motions and collisions is denoted by the granular temperature. Most of the mechanical energy of the solid particles is in the form of kinetic energy manifested as the random motion. In case of elastic collisions the entire energy is remains within the particles but in case of inelastic collisions the collisions are imperfect and some of the energy is lost in the form of sound and heat.

The equation for kinetic energy conservation is given as follows

$$\frac{3}{2}\left[\frac{\partial(\rho_s \varepsilon_s \theta_s)}{\partial t} + \nabla.(\rho_s \varepsilon_s \theta_s \nu_s)\right] = (p_s I + \tau_s):\nabla \nu_s + \nabla.(k_s \nabla \theta_s) - \gamma_s + \phi_{gs} \qquad (3.16)$$

The expression for coefficient for diffusion granular energy (k_s) was developed from the kinetic theory of granular flow given by Gidaspow is as follows:

$$k_s = \frac{(150\ \rho_s\ d_s \sqrt{\theta_s\ \pi})}{384\ (1+\varepsilon_{ss})\ g_{0,ss}} [1+\frac{6}{5}\alpha_s\ g_{o,ss}\ (1+e_{ss})]^2 + 2\varepsilon_s\ \rho_s\ g_o\ (1+e)\ (\frac{\theta_s}{\pi})^{0.5} \qquad (3.17)$$

The collision dissipation accounts for the inelastic collisions and the loss of energy due to this (γ_s) is given by the following expression from:

$$\gamma_s = \frac{12(1-e^2)g_0}{d_s\ \sqrt{\pi}} \rho_s \varepsilon_s \theta_s \nu_s \qquad (3.18)$$

The kinetic energy transfer function (ϕ_{gs}) is expressed as:

$$\phi_{gs} = -3K_{gs}\theta_s \qquad (3.19)$$

Drag Models

The force of drag exerted by the gas on the solid particles is defined by various laws Gidaspow gave the expression for drag laws most commonly used for solid-gas. It consists of two laws one when the solid fraction is low and the other when the solid fraction is high. In the dense zone $\varepsilon_g <= 0.8$ Ergun's equation is used to calculate the pressure drop and for the dilute phase $\varepsilon_g > 0.8$ the model used is given by Wen and Yu.

The Wen and Yu equation is as follows

$$K_{gs} = \frac{3}{4} C_D \{\varepsilon_s * \rho_s * \varepsilon_g * (\upsilon_s - \upsilon_g) / d_s\} \varepsilon_g^{-2.65} \quad (3.20)$$

The drag coefficient is given by the following expression

$$C_D = \frac{24}{Re}(1+0.15Re^{0.687}), Re<1000 \quad (3.21)$$

$$C_D = 0.44, \quad Re => 1000$$

Renolyds Number(Re) for the particles is calculated by the following expression

$$Re = [\rho_g * d_s * (\upsilon_s - \upsilon_g) / \mu_g] \quad (3.22)$$

$$K_{gs} = 150(\varepsilon_s \varepsilon_s \mu_g / \varepsilon_g d_s d_s) + 1.75[\varepsilon_s \rho_g (\upsilon_s - \upsilon_g) / d_s] \quad (3.23)$$

Reaction model

Methane reforming consists of a number of complex reactions occurring in parallel whose rate depends on the catalyst used and the conditions of the reaction. The main products are carbon monoxide and hydrogen. Along with the reforming reactions coke formation also occurs to some extent along with the Shift reaction. The major reactions occurring are as follows

$CH_4 + 2O_2 \rightarrow CO_2 + 2H_20$

$CH_4 + H_2O \rightarrow CO + 3\ H_2$

$CH_4 + CO_2 \rightarrow 2CO + 2H_2$

$CO + H_2O \rightarrow CO_2 + H_2$

All the reactions are modeled by laminar finite rate. The rate kinetics are defined by Arrhenius model and the kinetic parameters are found from literature. All the reaction occur in the fluidized bed and the species conservation equation for each species is given as follows

$$\frac{\partial}{\partial t}(\rho_i X_i) + \nabla.(\rho_i \upsilon_i X_i) = -\nabla J_i + R_i \quad (3.24)$$

the diffusive flux of the species i is expressed as

$$J_i = -\rho_i D_i \nabla X_i \quad (3.25)$$

R_i is the source term (rate of formation)

CHAPTER 4

SOLUTION METHODOLOGY

4.1 Problem Statement

The simulation of oxidative methane reforming was done in a fluidized bed reactor with the help of CFD technique using fluent software. The dimensions of the reactor are 2 m in height and 0.1 m inside diameter. The unfluidized bed is of 0.5 m height with a void fraction of 0.4. The catalyst is alumina based nickel catalyst and all the particles are considered to be spherical and of uniform size. The fluidization of the catalyst bed is carried out by the reactant gases entering at the bottom of the reactor. The reactions occur at the surface of the catalyst and some volumetric reactions also occurs. For uniform distribution of the gases inside the reactor the gas is introduced from three inlets each having a diameter of 0.01 m. The reaction is carried out adiabatically in the reactor and the outlet pressure is set to different pressures depending upon the reaction conditions. The product gas is composed of CO, CO_2, CH_4, H_2 and N_2.

Table 4.1: Reactor Setup

Reactor Setup	Value
Height	2.0 m

Width	0.1 m
Solid Phase	Value
Size (diameter)	186 um
Density	2270 kg/m^3
Initial Bed Height	0.5m
Initial Void Fraction	0.4

4.2 Numerical Methodology

To simulate the reforming reactions of methane the Eulerian Eulerian model is used. All the reactions are simulated using the laminar finite rate model for the volumetric reactions and heterogeneous reactions occur at the catalyst surface.

Geometry and grid

The fluidized bed is of dimensions 2 m in height and 0.1 m in width . The grid was created using CAD software GAMBIT. The mesh created using GAMBIT is exported to ANSYS FLUENT 14.5. The initial solid packing and the Grid is shown in the figure below is shown in below.

Simulation set up

The primary phase is mixture consisting of methane, oxygen, carbon dioxide, carbon monoxide , hydrogen , water vapor, nitrogen. The gases are assumed to be ideal and incompressible. The secondary phase is the Nickel/ alumina catalyst of constant density and uniform particle size.

The equations are solved by finite volume approach using second order upward discretization schemes. The reactions are described by the reaction kinetics and kinetics parameters taken from literature.

Table 4.2: 2D grid of the reactor

No. of cells	10376
No. of faces	5924
No. of nodes	9765
Cells	Trigonal

Table 4.3: Operating and boundary conditions

Inlet boundary condition	Velocity inlet
Outlet boundary condition	Pressure outlet
Wall boundary condition	No slip
Acceleration due to gravity	-9.81 m/s^2

Table 4.4: Simulation setup

Time step size	0.01s
Convergence criteria	0.0001
Discretization method	Second order upwind
Drag law	Gidaspow
Coefficient of restitution	0.95
Granular Bulk Viscosity	Lun-et al.
Granular conductivity	Gidaspow et al.
Solid pressure	Lun et-al

Kinetic parameters for reactions

$$CH_4 + 2O_2 \longrightarrow 2H_2O + CO_2 \quad [\Delta H^0_{298} = -802 \text{ kJ/mol}] \qquad (1)$$

$$CH_4 + H_2O \longrightarrow CO + 3H_2 \quad [\Delta H^0_{298} = 206 \text{ kJ/mol}] \qquad (2)$$

$$CH_4 + CO_2 \longrightarrow 2CO + 2H_2 \quad [\Delta H^0_{298} = 247 \text{kJ/mol}] \qquad (3)$$

$$CO + H_2O \longrightarrow CO_2 + H_2$$

the rates of the above reactions are given by the following correlation

$$r_1 = k_3 P_{CH4} P_{H2O} \left(1 - \frac{P^3_{CH_4} P_{CO}}{K_2 P_{CH_4} P_{CO_2}}\right)$$

$r_2=k_2 P_{CH4} P_{CO2}(1-\frac{P_{H2}^2 P_{CO}^2}{K_2 P_{CH4} P_{H20}})$

$r_3=k_3 P_{CH4} P_{CO2}(1-\frac{P_{H2}^2 P_{CO}^2}{K_3 P_{CH4} P_{CO2}})$

k_1= 3.96 x10^9exp(-$\frac{166}{RT}$) (kmol/kPa^2.kgcat.h)

k_2= 15.08 exp(-$\frac{29}{RT}$) (kmol/kPa^2.kgcat.h)

k_3= 8.71 exp(-$\frac{23.7}{RT}$) (kmol/kPa^2.kgcat.h)

K_2=exp(-$\frac{26262}{T}$ + 38.9)(kPa^2)

K_3=exp(−$\frac{30782}{T}$ + 42.970)(kPa^2)

CHAPTER 5

RESULTS AND DISCUSSIONS

The equations described in the earlier section are solved by the CFD simulation software FLUENT 14.5 (ANSYS). The results obtained from the simulation are presented below

5.1 Hydrodynamics Of Fluidized Bed

The interaction of the two phases is investigated in the hydrodynamics of the reactor. The drop of pressure across the reactor, and the results obtained by hydrodynamic studies is presented below.

5.1.1 Pressure drop across the bed

From theoretical and experimental studies the pressure drop across the bed increases continuously with increase with the increase of superficial velocity until minimum fluidization is achieved after that the pressure drop remains invariant with the increase of velocity. There is some amount of variation with time due to the continuous fluctuation in the position and distribution of the phases due to the bubbling in the bed. The average pressure drop can be obtained from the force balance and the expression is as follows

$$\Delta P=(\rho_s-\rho_g)(1-\varepsilon_{mf})gL \quad (5.1)$$

L= bed height

ε_{mf} = void fraction at minimum fluidization condition.

ρ_s and ρ_g are the solid phase and gas phase density.

The theoretical value of pressure drop is found out to be

$$\Delta P=(\rho_s-\rho_g)(1-\varepsilon_{mf})gL$$

$=\rho_s(1-\varepsilon_{mf})gL$,Since the density of gas is negligible compared to the solid catalyst

=2270*(1-0.6)*9.81*0.5 Pa

=4453.74 Pa

5.1.2 Contours of Pressure drop and volume fraction of solid phase in the reactor

The contours of solid phase in the reactor helps to analyze the distribution of gas and solid phase in the reactor. Fig 5.1-3 gives the contours of volume fraction of the solid phase at different times and different velocities. The Fig gives the contour of the velocity across the reactor at different velocities.

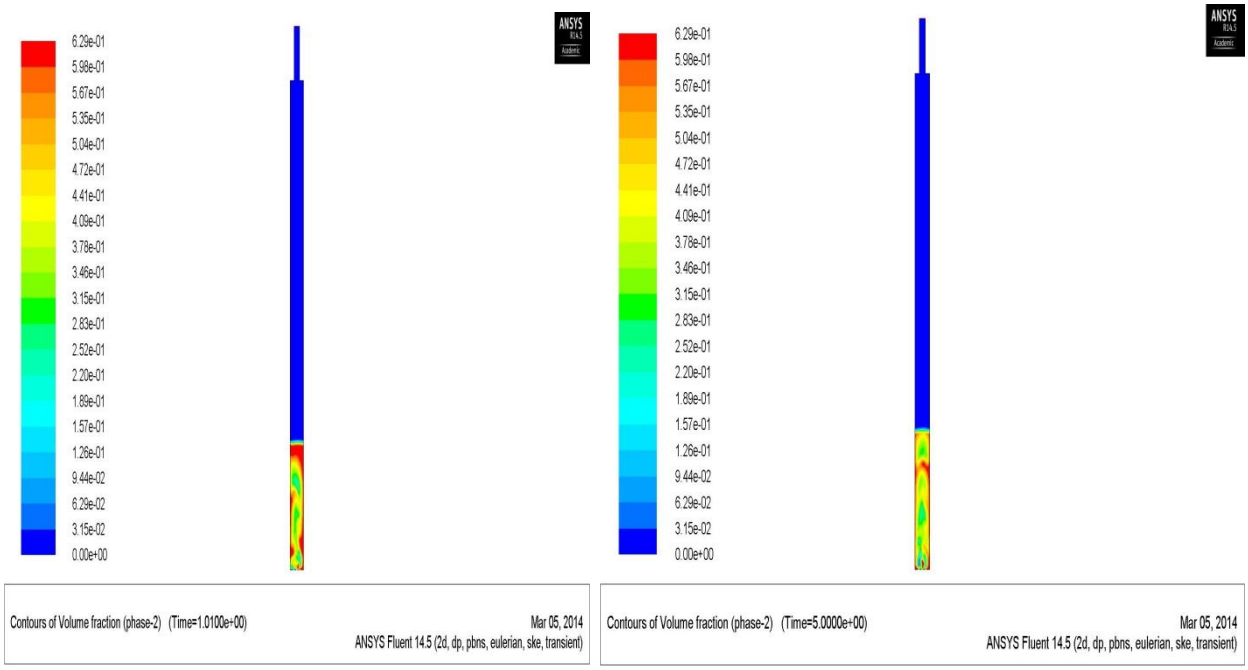

Fig 5.1 (a) **Fig 5.1 (b)**

Fig 5.1 (a): Contours of volume fraction of solid phase at 1s and superficial velocity of 0.6 m/s.

Fig 5.1 (b): Contours of volume fraction of solid phase at 5s and superficial velocity of 0.6 m/s.

From figure 5.1(a) and Fig 5.1(b) it is can be seen that there is very little variation in bed height with time although the distibution of the solid may change with time.

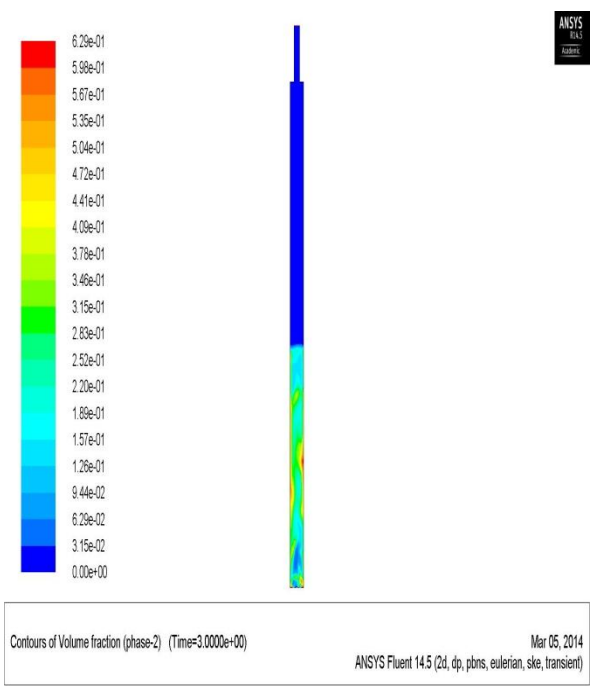

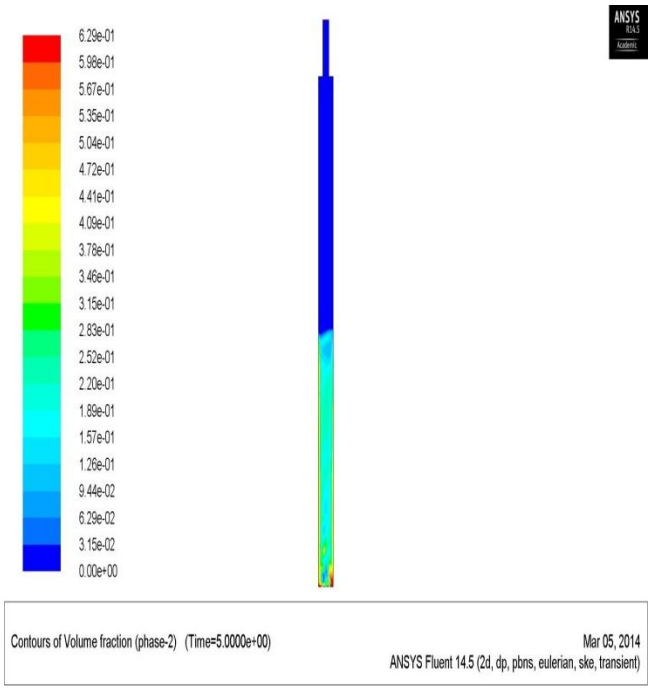

Fig 5.2 (a) **Fig 5.2(b)**

Fig 5.2(a): Contours of volume fraction of solid phase at 3s and superficial velocity of 0.9 m/s.

Fig 5.2 (b): Contours of volume fraction of solid phase at 5s and superficial velocity of 0.9 m/s.

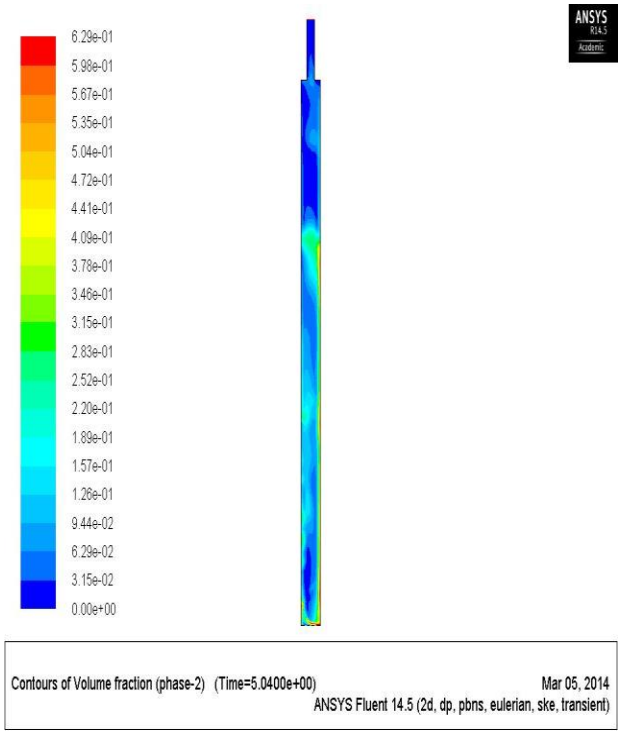

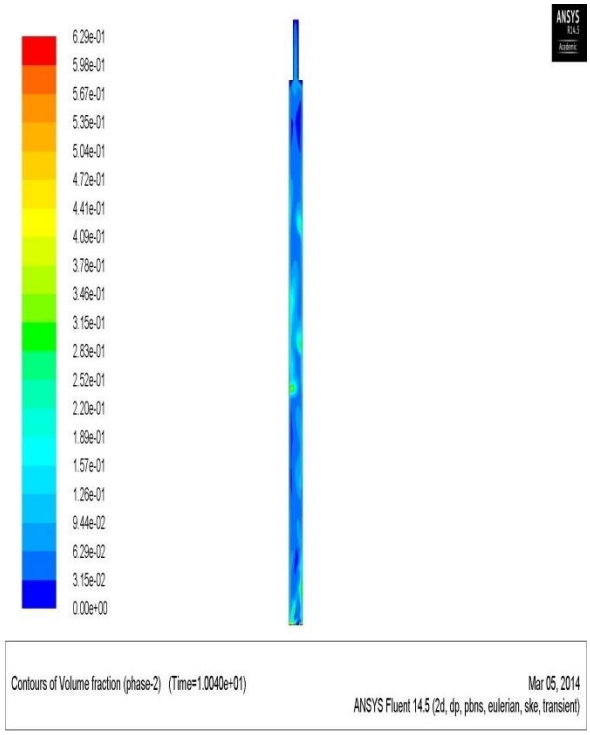

Fig 5.3(a) **Fig 5.3 (b)**

Fig 5.3(a): Contours of volume fraction of solid phase at 5s and superficial velocity of 1.2 m/s.

Fig 5.3 (b): Contours of volume fraction of solid phase at 10s and superficial velocity of 1.2 m/s.

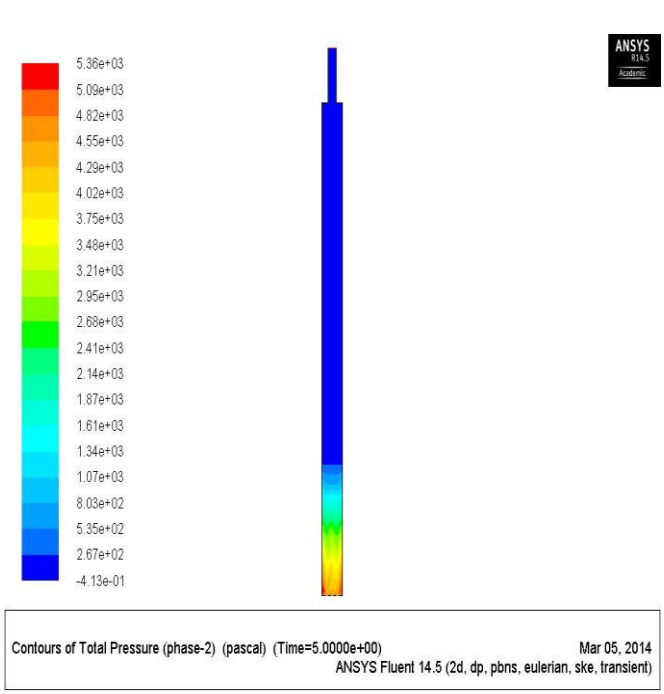

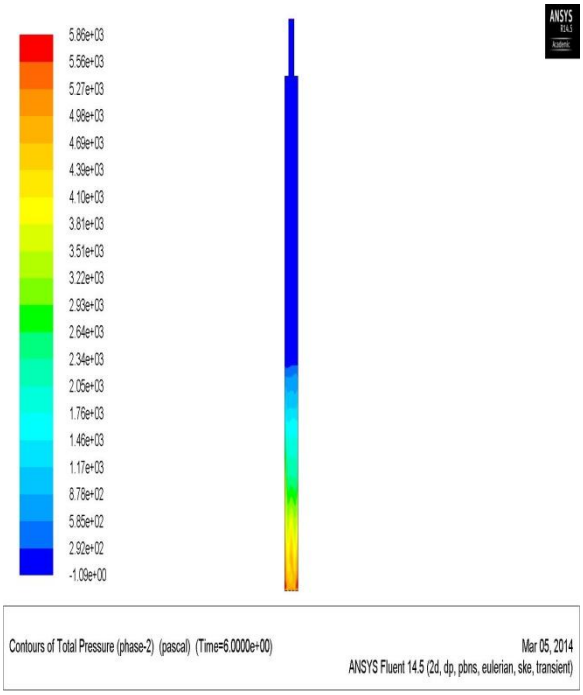

Fig 5.4 (a) **Fig 5.4 (b)**

Fig 5.4(a): Contours of gage pressure at 5s and superficial velocity of 0.6 m/s.

Fig 5.4 (b): Contours of gage pressure at 10s and superficial velocity of 0.9 m/s.

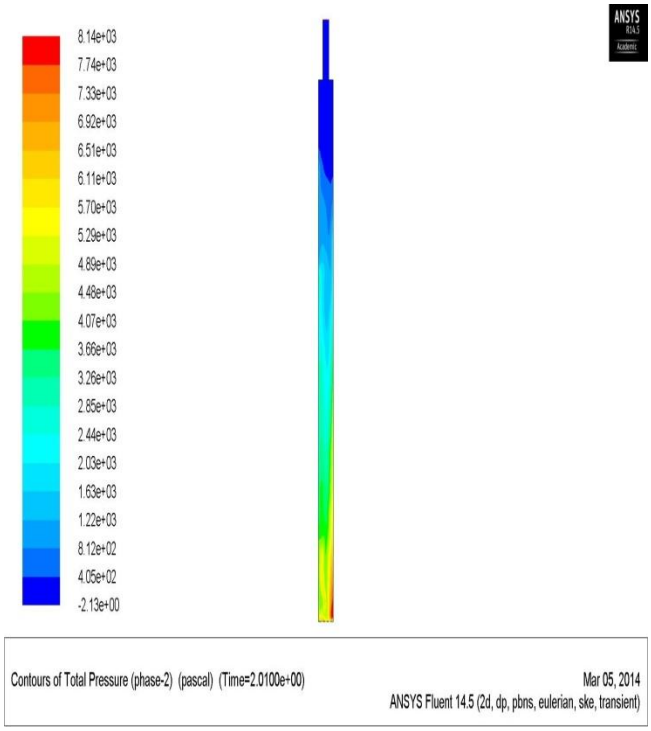

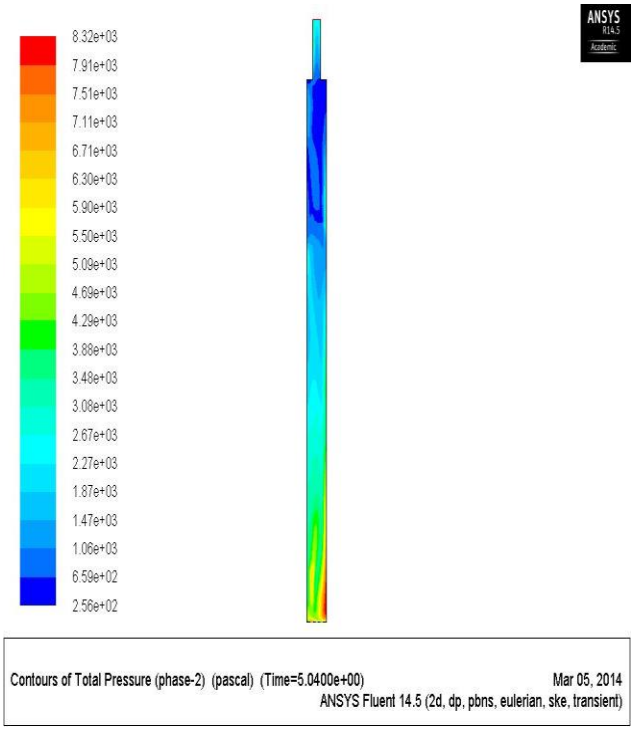

Fig 5.5 (a) **Fig 5.5 (b)**

Fig 5.5(a): Contours of gage pressure at 2s and superficial velocity of 1.2m/s.

Fig 5.5(b): Contours of gage pressure at 5s and superficial velocity of 1.2 m/s.

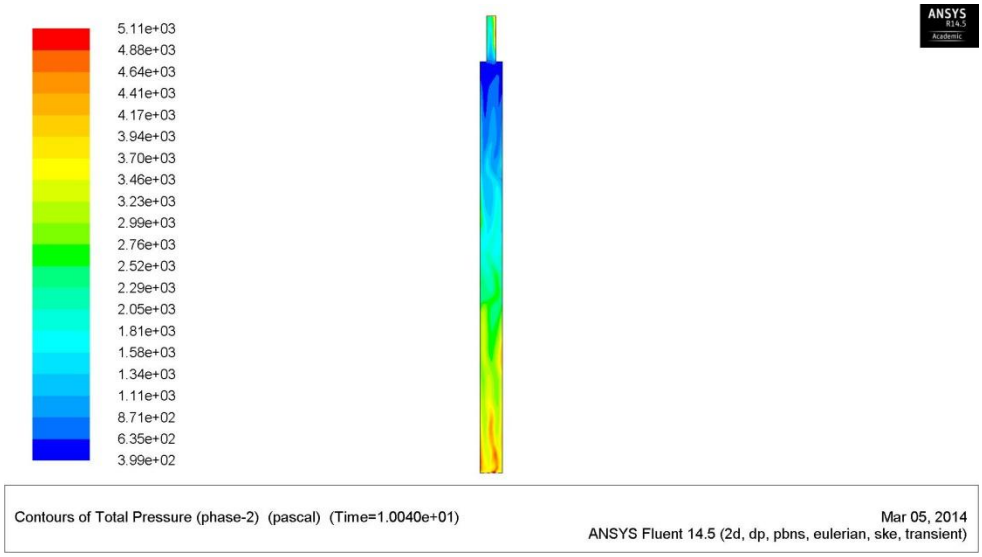

Fig 5.6

Fig 5.6: Contours of gage pressure at 10s and superficial velocity of 1.2 m/s

Table 5.1: Superficial velocity vs. pressure drop

	Superficial Velocity(m/s)	Area averaged Pressure Drop (Pa)
1.	0.60	4648
2.	0.9	4574
3.	1.2	4556

Table 5.2:Superficial velocity vs. time

Superficial velocity (m/s)	TIme (s)	Pressure drop(Pa)
0.6	1	4648
0.6	2	4636
0.6	5	4631

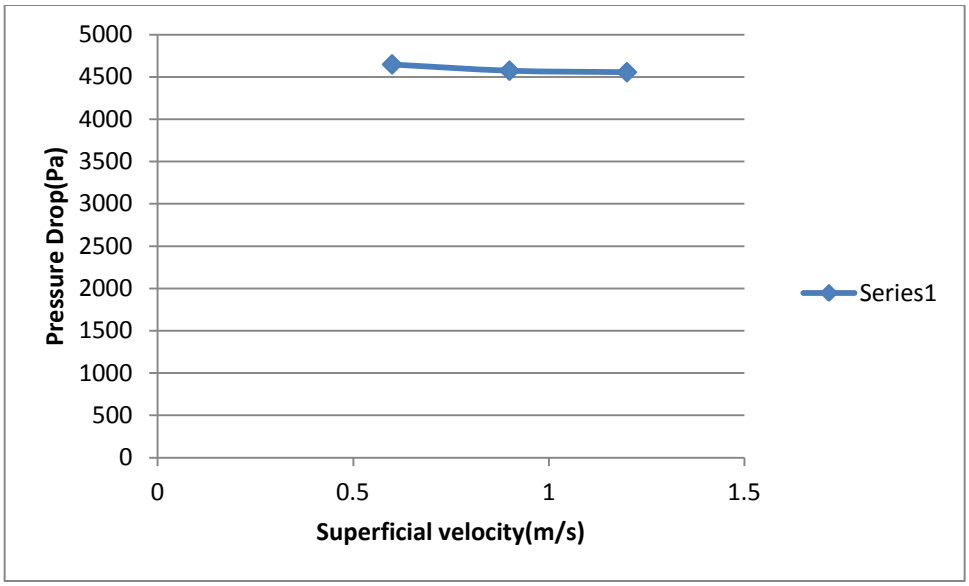

Fig 5.7: Variation of pressure drop with superficial velocity

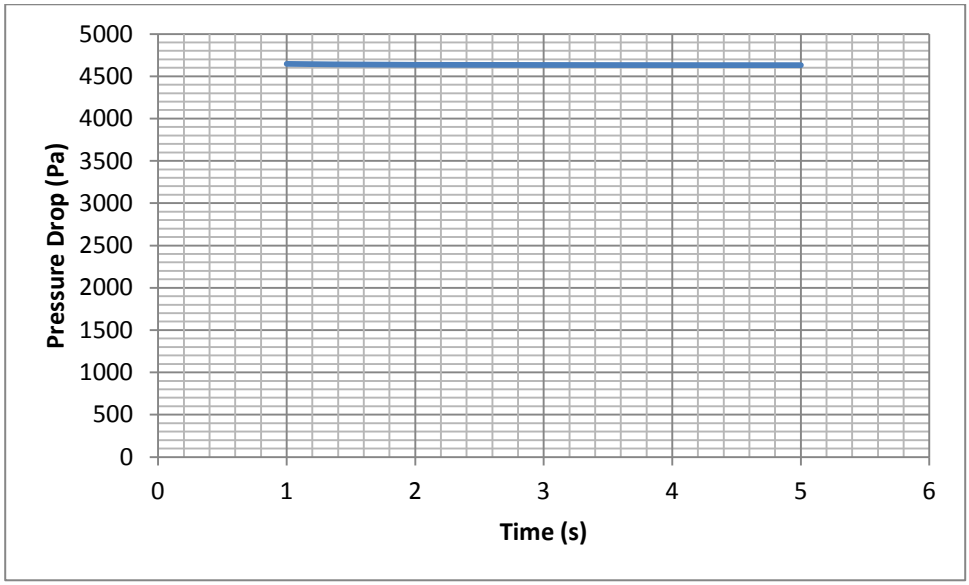

Fig 5.8: Variation of pressure drop with time (superficial velocity=0.6 m/s)

5.2 Reactant Conversion and Product Yield

In order to simulate the reforming reactions several reactions are incorporated occurring in parallel and series. The reactions are modeled along with the reverse reaction taking place except the combustion reaction because the reverse reaction is almost negligible for it. As the coking reaction is very small and the simulation is studied only till steady state is reached the coking reaction is neglected.

The performance of the reactor is determined by the methane conversion, H_2/CO ratio and Hydrogen Yield

In the reactor the Methane is converted into Carbon Dioxide, Carbon Monoxide, Water, Hydrogen. The product gas also consists of some amount of unconverted Methane, Oxygen and Nitrogen.

Conversion

The conversion at outlet of any species in the feed can be calculated as:

$$\text{Conversion } (X_i) = \left(1 - \frac{(C_i * \upsilon_i * A)_{inlet}}{(C_i * \upsilon_i * A)_{outlet}}\right) * 100 \qquad (5.2)$$

Where C_i is the concentration of the i^{th} species

υ_i is the velocity of the i^{th} species which is same as average velocity at inlet or outlet.

A is the area of the inlet or the outlet.

H_2/CO ratio

The primary products of the reforming are hydrogen and carbon monoxide. The Hydrogen to Carbon monoxide is important because a lower ratio is desirable for further use of syngas as feed for Fisher Tropsh process and a higher ratio is desirable for industries where the main feed is hydrogen.

Hydrogen to Carbon Monoxide ratio is defined as: $\frac{C_{H_2 outlet}}{C_{CO outlet}}$ (5.3)

Hydrogen Yield The main purpose of the reforming reaction is the formation of hydrogen which is separated from CO for use in various chemical industries or is used along with it for processes like FT process. The hydrogen yield is defined as follows:

$$\frac{(C_{H_2} * \upsilon_{H_2} * A)_{outlet}}{((C_{CH_4} * \upsilon_{CH_4} * A)_{inlet})} \quad (5.4)$$

5.3 Validation of Model

The results obtained through the reforming of methane in a fluidized bed reactor were in good agreement with results obtained by Abashar et al.[

The deviation of simulated results from the previous studies are within limits of error

Table 5.3: Comparison of results

	Simulations	Abashar et al
Catalyst	Ni/Al203	Ni/Al203
Feed Temperature	673 K	673 K
O_2/CH_4 mole ratio	0.1	0.1
Product Composition		
CH_4 Conversion	20.55	19.44
H_2 yield	0.453	.474
Outlet temperature	787 K	802 K
O_2/CH_4 mole ratio	0.3	0.3
CH_4 conversion	61.5	58.0
H_2 yield	1.303	1.22
Outlet temperature	910 K	918 K
O_2/CH_4 mole ratio	0.5	0.5
CH_4 conversion	99.3	96
H_2 yield	1.86	1.91
Outlet Temperature	1026 K	1038 K

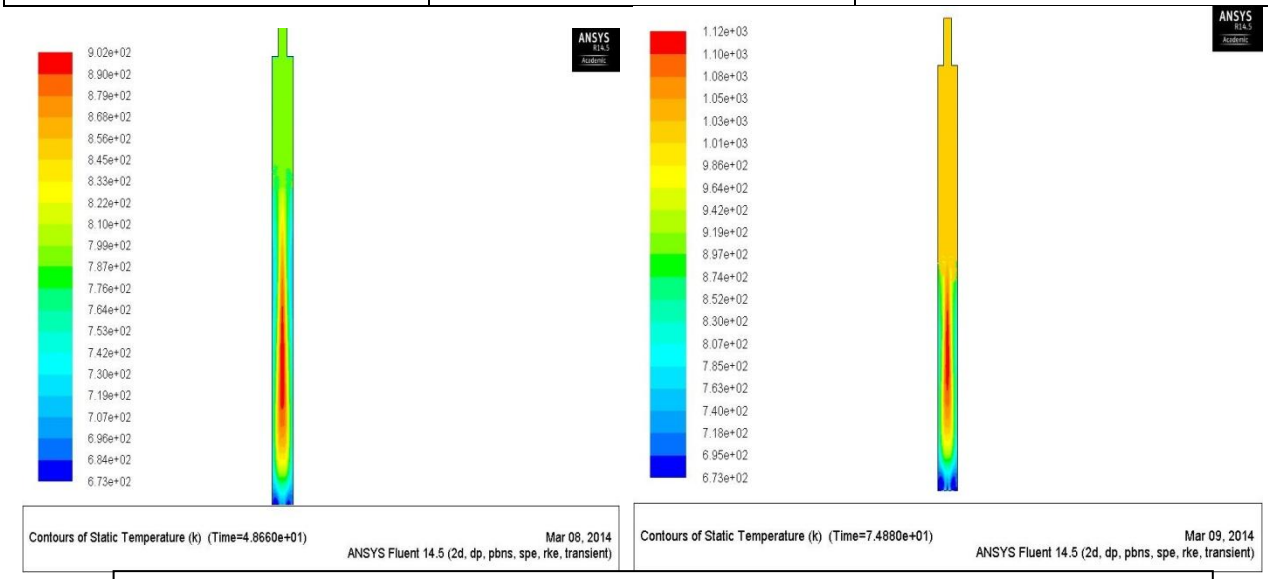

Fig 5.9(a): Contours of temperature O_2/CH_4 ratio =0.1, time= 48s

Fig 5.9(b): Contours of temperature O_2/CH_4 ratio =0.5, time= 74s

5.4 Effect of CO_2 addition

The dry reforming reaction is valuable because it eliminates two undesirable greenhouse gases at once and at the same time it gives lower H_2/CO ratio as compared to steam reforming so by addition of CO_2 along with oxygen for Oxidative reforming it is possible to optimize the H_2 production and the H_2/CO ratio.

5.4.1 Effect of CO2 Addition on productivity of Hydrogen

Table 5.4: CO_2 / CH_4 mole ratio vs. Hydrogen production(O_2/CH_4=0.5)

CO_2 / CH_4 Feed	Hydrogen Concentration at exit (mol/m3)
0.1	2.16
0.2	3.71
0.3	4.77
0.4	5.35
0.5	5.51

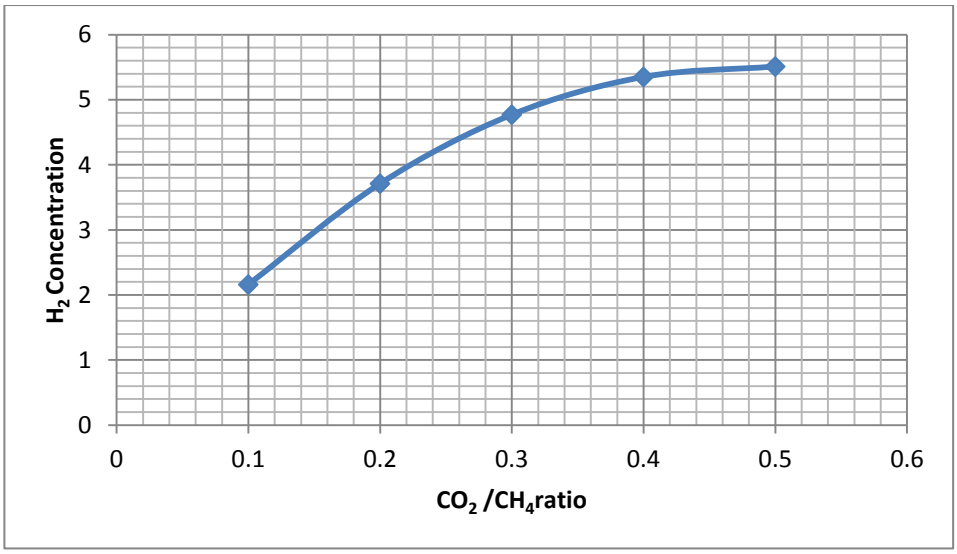

Fig 5.10: Variation of hydrogen production with CO_2 / CH_4 mole ratio(O_2/CH_4=0.5)

As shown in Fig 5.10 the Hydrogen concentration increases with the addition of CO_2 with the feed. This is because increased CO_2 addition favors the dry reforming process in accordance with Le Chateliers principle producing more Hydrogen. Another product of the dry reforming process is CO which takes part in shift reaction and leads to formation of more Hydrogen. The productivity increases rapidly and then increases at a slower rate as the mole ratio in the feed

approaches 0.5 this may be because the reverse shift reaction is favored as the concentration of CO_2 is further increased and near equilibrium conditions are achieved at these conditions because of increased rate of reactions.

5.4.2 Conversion profile of CH_4 along the length of the reactor

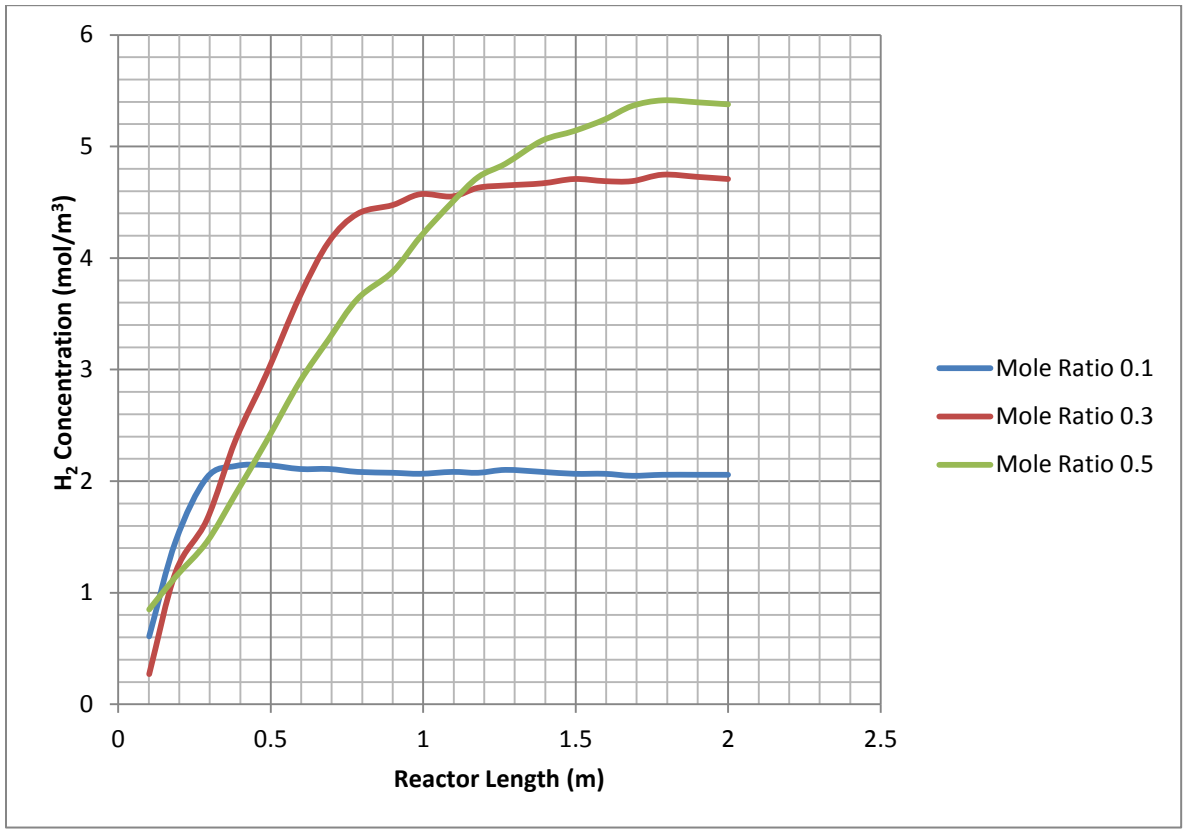

Fig 5.11: Variation of H_2 concentration along the length of the reactor at different mole ratio of CO_2/CH_4.

The above figure shows the variation of hydrogen concentration along the length of the reactor. For the mole ratio of 0.1 most of the reaction is completed in less than 0.5 m of the reactor length because of small amount of CO_2. As the concentration is increased the dry reforming occurs in the remaining portion of the reactor. The hydrogen concentration at exit increases from 2 mol/m^3 to 5.5 mol/m^3 and the reaction undergo completion after 1.75 m of reactor length.

5.4.3 Effect of CO2 addition on H_2/CO ratio in product.

Table 5.5 H_2/CO ratio product vs CO_2/CH_4 ratio Feed

CO_2/CH_4 ratio Feed	H_2/CO ratio product
0.1	1.423
0.2	1.56
0.3	1.664
0.4	1.727
0.5	1.785

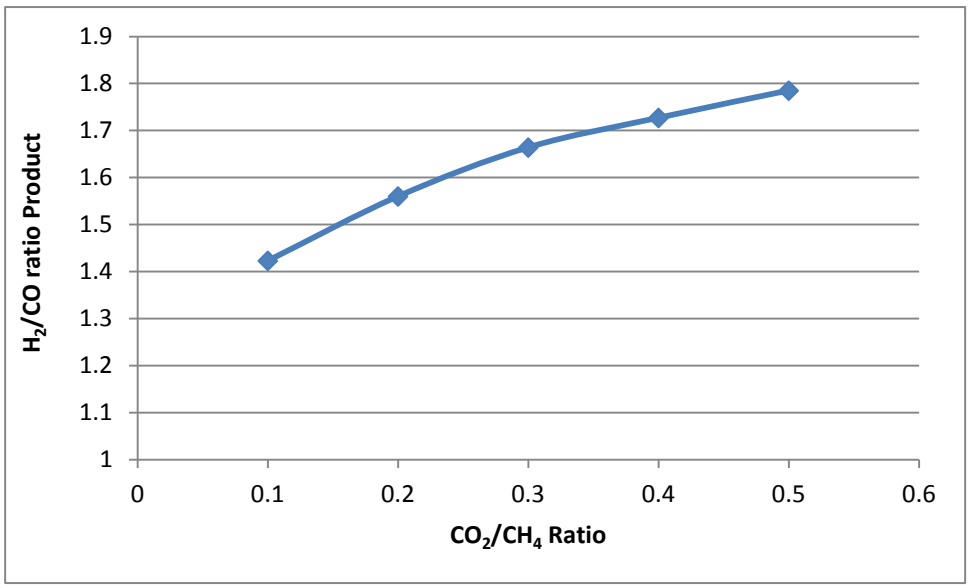

Fig 5.12: Variation of H_2/CO ratio with CO_2/CH_4 ratio in feed(O_2/CH_4=0.4)

From the Figure 5.12 we see that the H_2/CO ratio increases with the increase of CO_2/CH_4 ratio. This is because more CO is produced from the dry reforming reaction and this increased concentration of CO drives the water gas shift reaction forward producing more H_2 as a result of which the H_2/CO ratio is increased. As the carbon dioxide to methane ratio is increased from 0.1 to 0.5 the mole ratio increases from 1.423 to 1.785.

5.4.4 Conversion profiles of CH_4

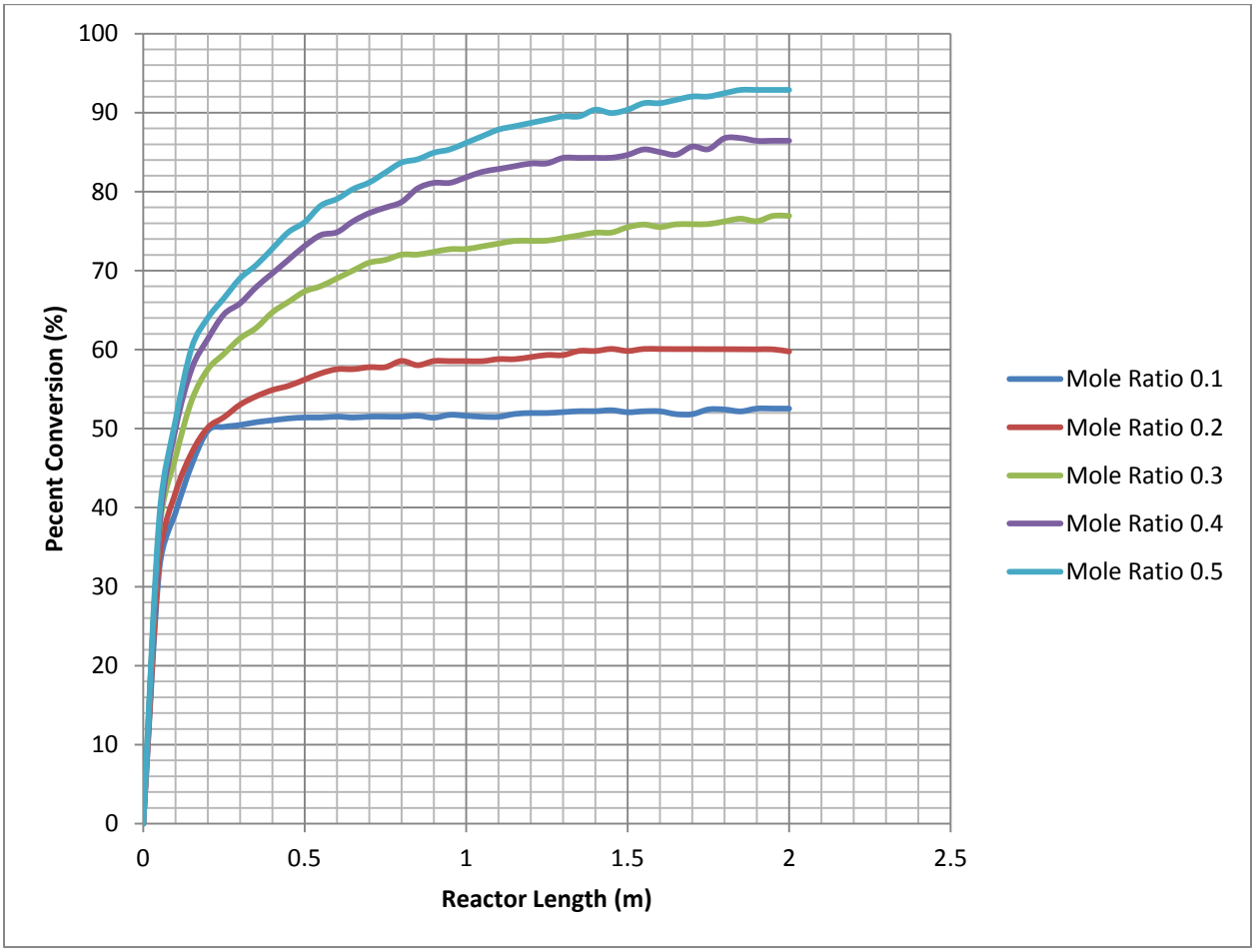

Fig 5.13: Profile of CH_4 conversion along the length of the reactor with CO_2/CH_4 ratio in feed(O_2/CH_4=0.4)

From Fig 5.13 it can be seen the methane conversion increases with increasing CO_2/CH_4 ratio in feed . We see that the conversion of about 50% of methane occurs rapidly due to the combustion of reaction then the rate of consumption decreases along the length of reactor as the conversion is due to steam reforming and dry reforming reactions which are slower than the combustion reaction. The conversion of methane reaches 93% for mole ratio of CO_2/CH_4 =0.5.

5.4.5 Variation of conversion with change in CO_2 mole fraction

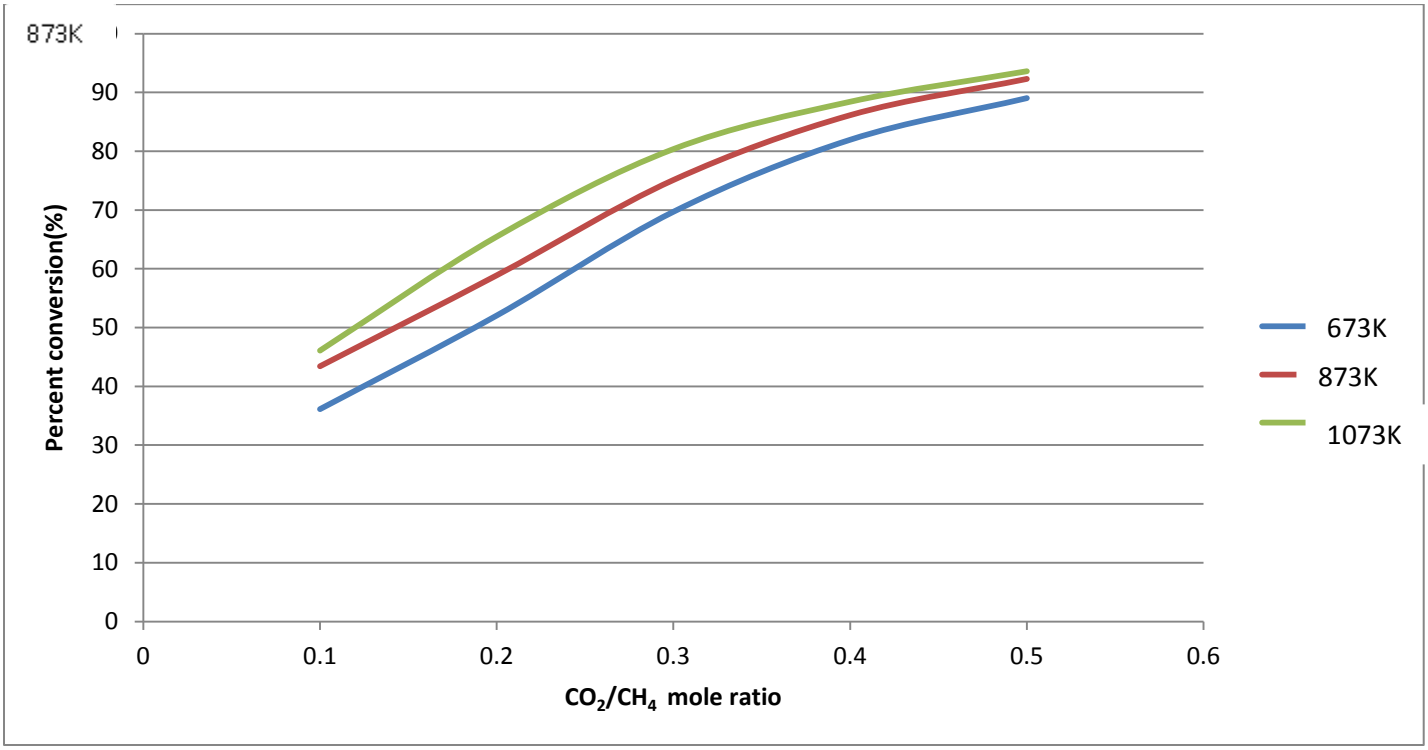

Fig 5.14: CH_4 conversion vs CO_2/CH_4 at different inlet temperatures. (O_2/CH_4=0.4)

Fig 5.14 shows the variation of the CH_4 conversion at different temperature with changing mole ratio of CO_2/CH_4. As the amount of CO_2in the feed is increased conversion of CH_4 is found to increase this is because of the increased rate of dry reforming reaction. The CH_4 conversion feed temperature of 673 K increases from 38% to 89% as the mole ratio is increased from 0.1 to 0.5. Also the conversion at any given mole ratio increases with increasing temperature because the reactions are endothermic and are promoted at high temperature. The above figure shows variation of concentration at three different temperatures and the conversion for all of them reaches to near 89-93% for all of them at a mole ratio of 0.5.

5.4.6 Profiles of H_2O concentration

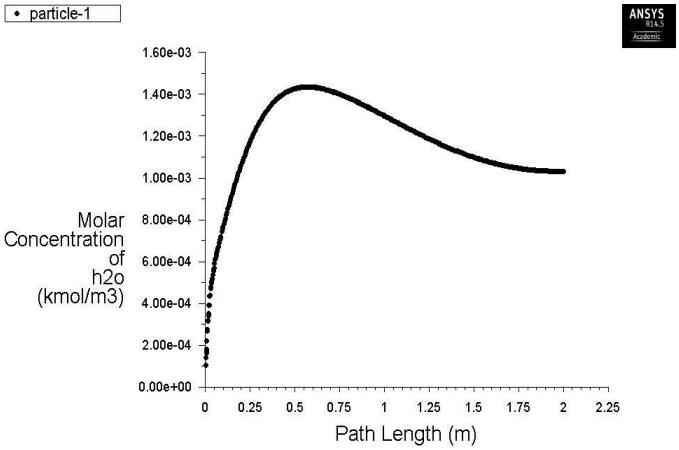

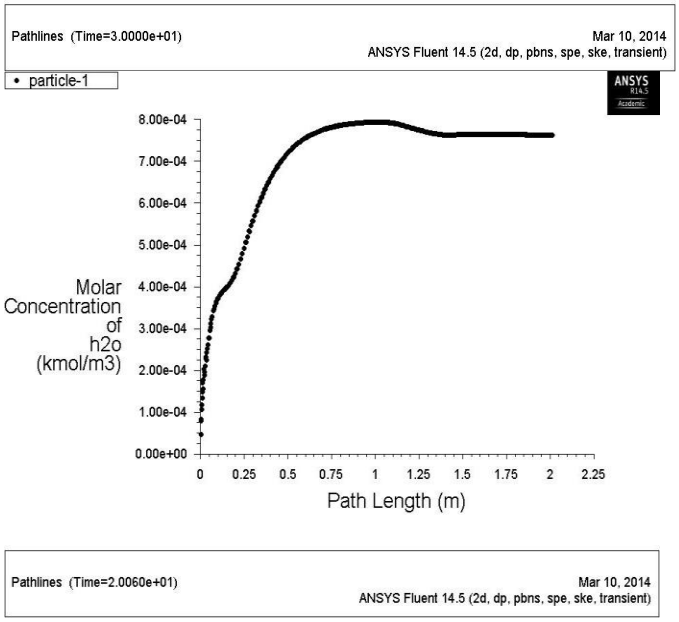

Fig 5.15(a) **Fig 5.15(b)**

Fig 5.15(a): H_2O concentration along length of reactor (CO_2/CH_4 =0.5)

Fig 5.15(b): H_2O concentration along length of reactor (CO_2/CH_4 =0.1)

From Fig 5.15 it can be seen that the H_2O concentration reaches as maxima and then decreases. The water is formed by combustion reaction of methane. The water then takes part in the water gas shift reaction forming H_2 and CO_2 as a result of which its concentration decreases. The decrease is more in

case of lower mole ratio of carbon dioxide to methane in the feed as more CO_2 promotes the rate of Reverse water gas shift reaction but H_20 is still consumed by the steam reforming reaction.

5.4.7 Temperature Profile along the length of reactor

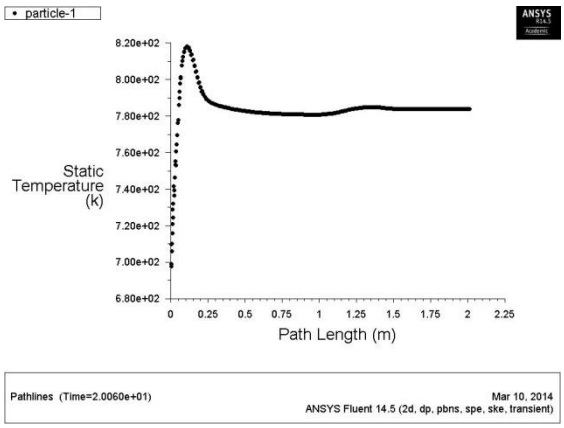

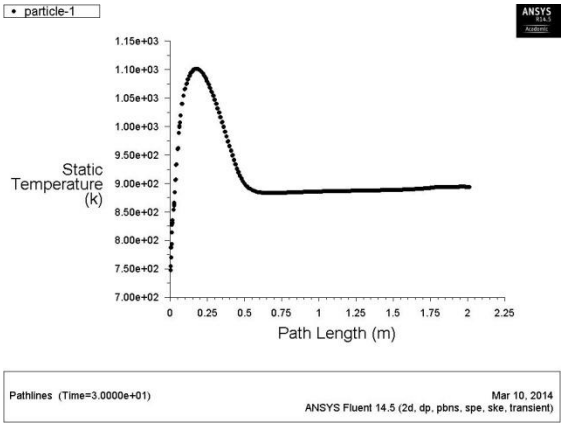

Fig 5.16 (a) **Fig 5.16(b)**

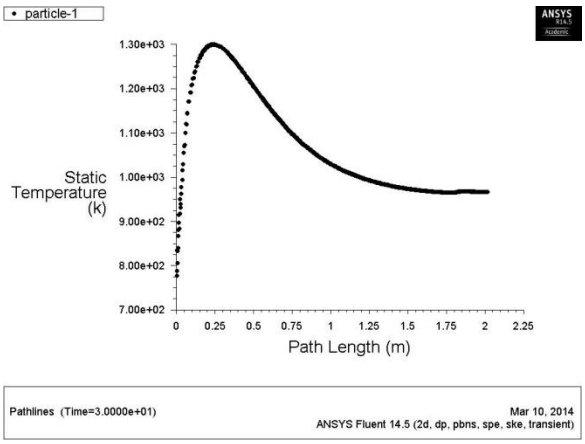

Fig 5.16(c)

Fig 5.16 (a): Profile of temperature along the length of reactor (O_2/CH_4 =0.1)

Fig 5.16 (b): Profile of temperature along the length of reactor (O_2/CH_4 =0.3)

Fig 5.16 (c): Profile of temperature along the length of reactor(O_2/CH_4 =0.5)

From the above figures we see that there is a formation of hotspot along the reactor length. The temperature of hotspot increases with the increasing CO_2/CH_4 ratio and reaches 1300 K for a mole ratio of 0.5. But the peak temperature reached is lesser in case of the fluidized bed as compared to fixed bed. As the mole ratio of Oxygen to methane is increased from 0.1 to 0.5 the peak temperature increases from 820 K to 1300K.The decrease from the peak temperature is lesser in case of the lower mole ratio because the reforming reaction occurring is lesser but as the amount of O_2 or CO_2 from combustion increases more reforming reaction occurs therefore the decrease from peak temperature is greater in this case.

5.4.8 Profiles of reaction along the length of reactor

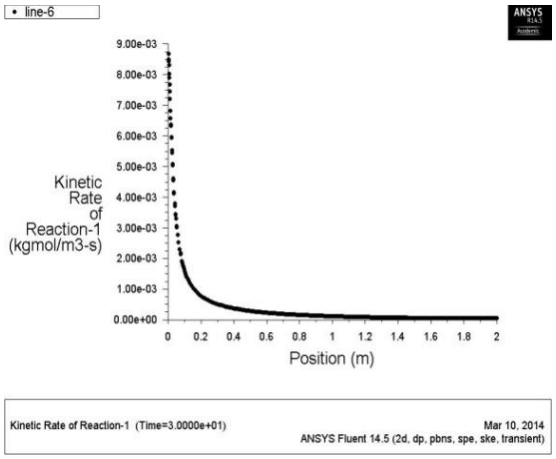

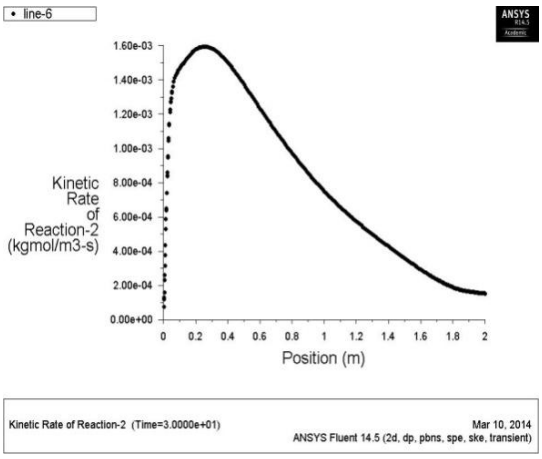

Fig 5.17 (a) **Fig 5.17(b)**

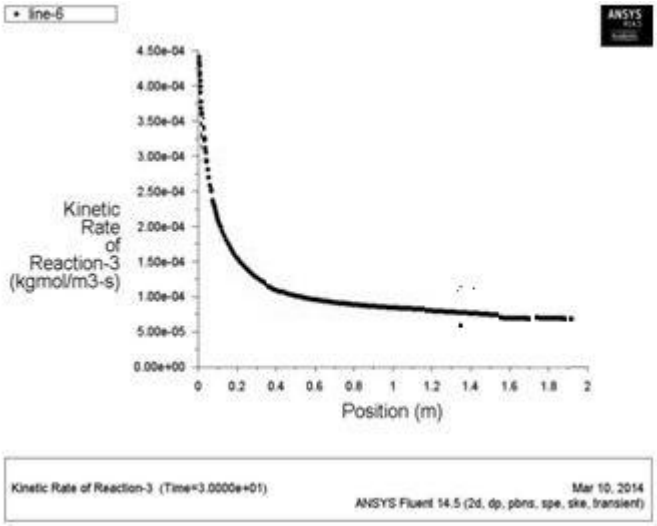

Fig 5.17(c)

Fig 5.17 (a): Profiles of combustion reaction along length of reactor

Fig 5.17(b): Profile of steam reforming reaction along length of reactor

Fig 5.17 (c): Profile of dry reforming reaction along length of reactor

The above figures show the rates of combustion, steam reforming and dry reforming reaction along the length of the reactor. The rates of combustion reaction decreases continuously along the length of the reactor as the methane and oxygen concentration decrease. The rate of reaction becomes negligible at the reactor exit. The rate of steam reforming reaction increases along the length of the reactor at first due to the formation of steam from the combustion reaction but decreases subsequently as the methane and steam are consumed in the reforming and shift reactions. The rate of dry reforming reaction also deceases along the length of the reactor .

5.5 Effect of Inlet Temperature

5.5.1 Effect of temperature on hydrogen production

Table 5.6: Hydrogen production vs. Inlet temperature

Inlet Temperature (K)	Concentration of H2 at outlet(mol/m^3)
673	2.16
873	2.85
1073	3.38

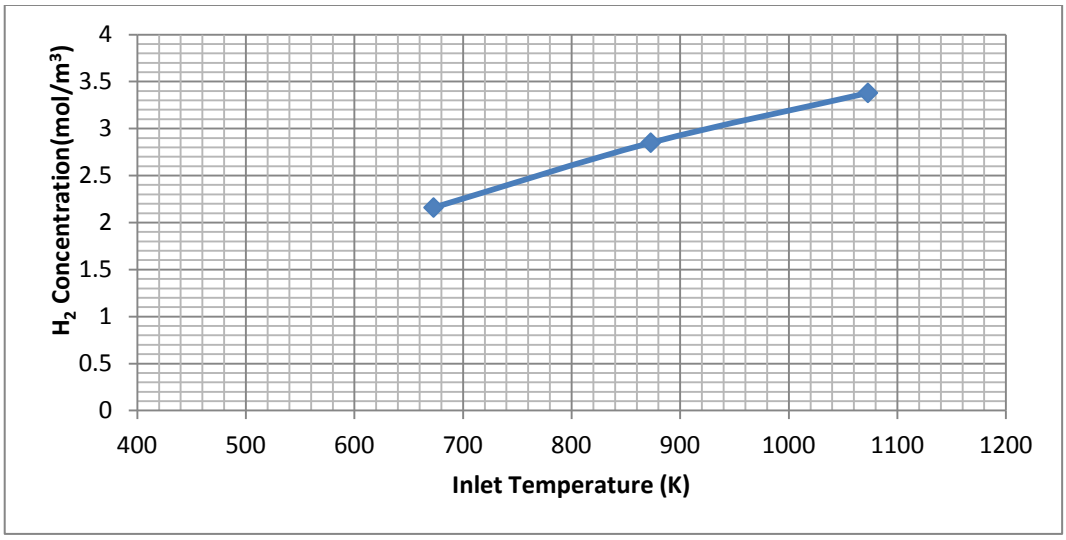

Fig 5.18: Variation of hydrogen production with inlet temperature ($CO_2/CH_4/ O_2$=0.1:1:0.5)

From 5.18 it is seen that the hydrogen concentration at the exit increases from 2.1 to 3.4(mol/m3) as the inlet temperature of the reactant gases is increased from 2.1 to 3.4 mol/m3 as the inlet temperature is increased from 673K to 1073K. This is explained by the fact that more energy is available for the reforming reactions as both the reforming reaction are endothermic in nature. Also with the increase of temperature the equilibrium constant increases for the endothermic reactions so the rate of the forward reactions for the reforming reactions increases as compared to the reverse reaction.

5.5.2 Variation of conversion with change in Temperature

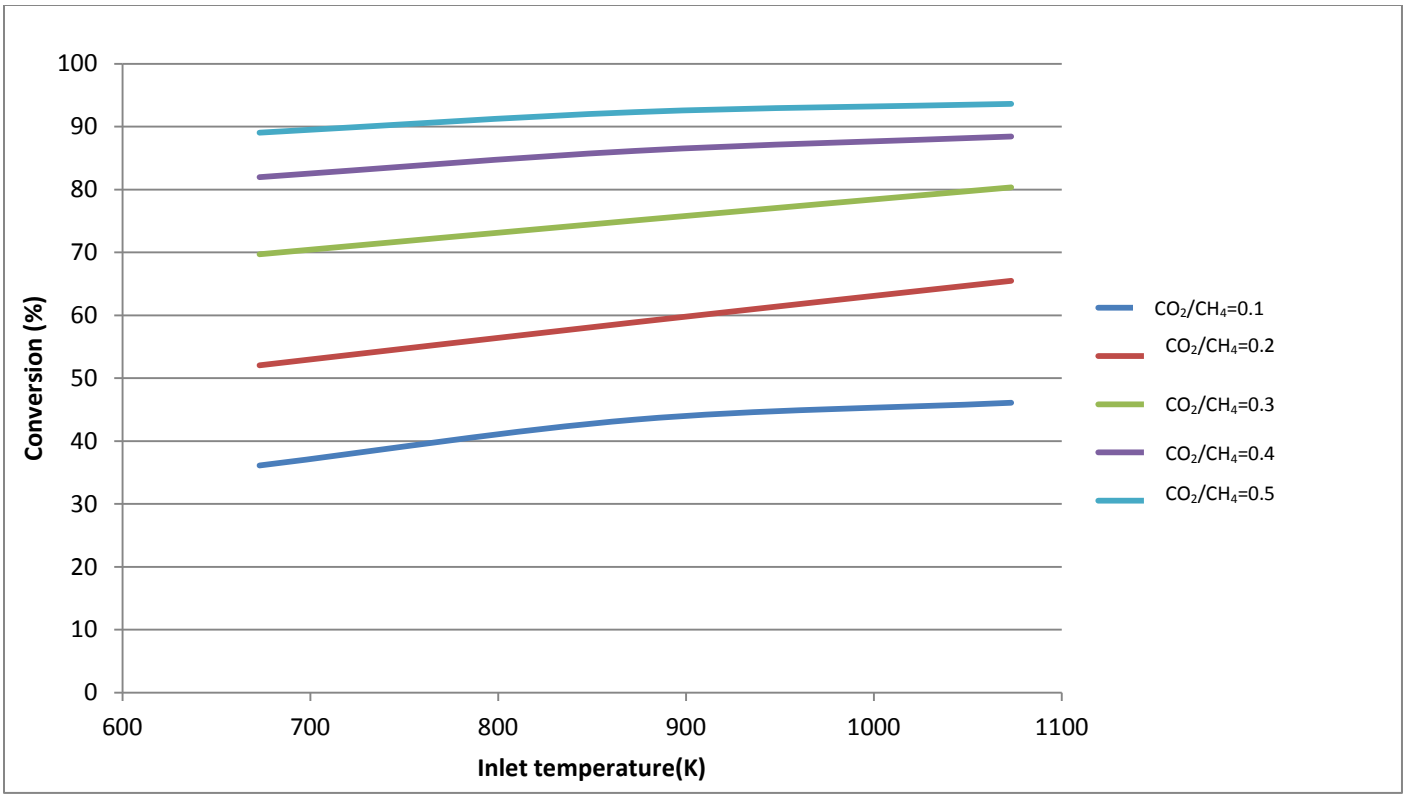

Fig 5.19: CH_4 conversion vs Temperature at different mole ratios of CO_2/CH_4 (O_2/CH_4=0.3)

Fig 5.19 shows the change in the variation in the conversion with inlet temperature at a fixed mole ratio. As the inlet temperature is increased the conversion increases. But we see that the increase is more at a lower mole ratio as compared to the increase at higher temperature. This may occur as at higher concentration the rate of reaction is already high and the reaction occurs fast and approaches to equilibrium conditions but at lower concentration the rate is slow and the rate of forward reaction and equilibrium constants are enhanced at higher temperature.

5.5.3 Effect of inlet temperature on exit temperature

Table 5.7 : Inlet temperature vs. exit temperature

Inlet Temperature(K)	Outlet Temperature(K)
673	790
873	815
1073	846

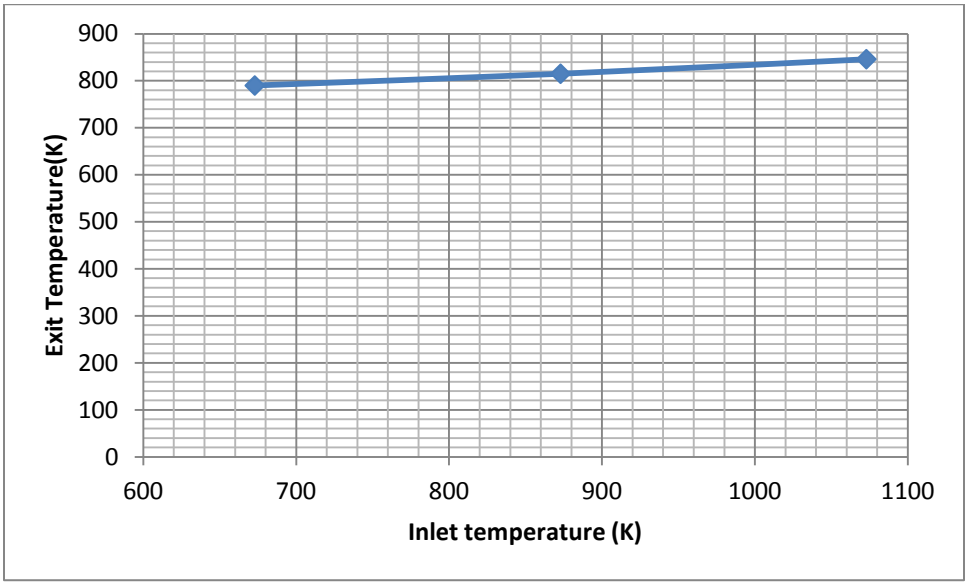

Fig 5.20: Variation of exit temperature with inlet temperature ($CO_2/CH_4/ O_2$=0.1/1/0.5)

As the inlet temperature is increased from 673K to 1073K the outlet temperature increases from 790 K to 850K only this is because much of the energy put into the system as heat is consumed in the reforming reactions which are endothermic in nature. This is evident as the hydrogen production increases with increase in inlet temperature.

5.5.4 Effect of inlet temperature on H_2/CO mole ratio

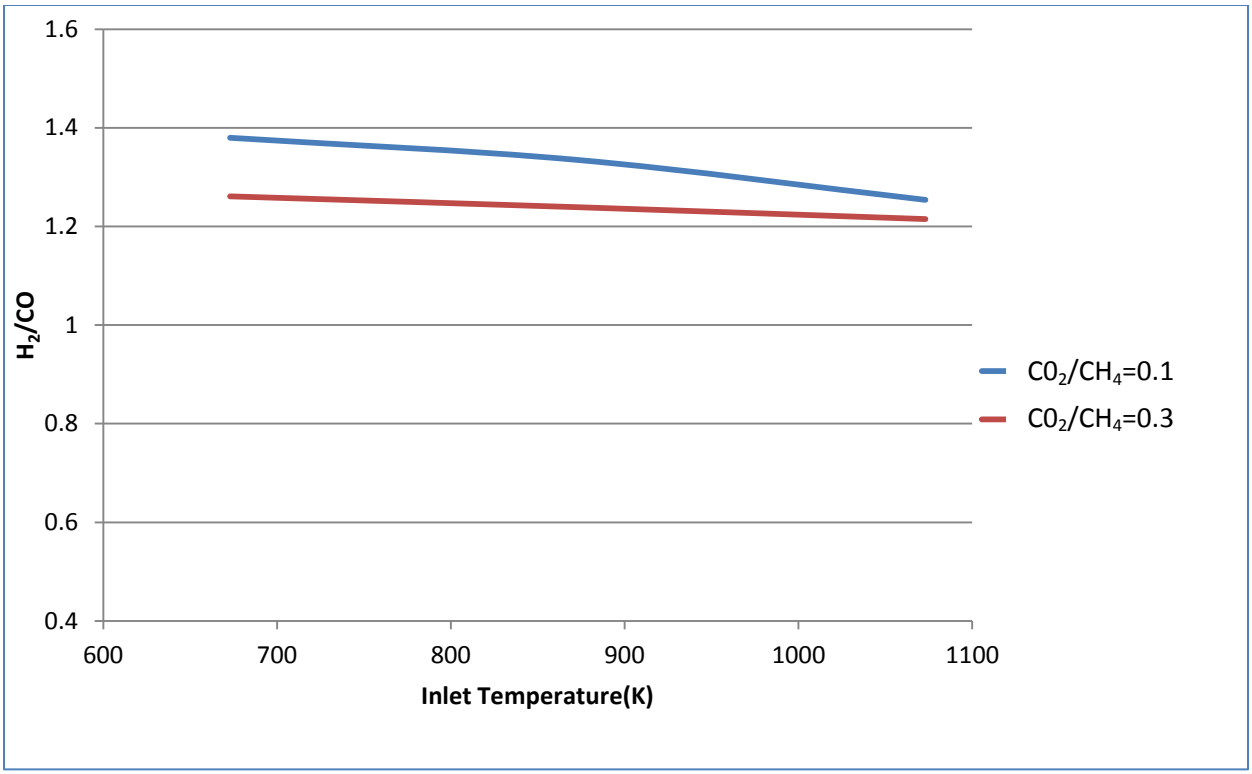

Fig 5.21: H_2/CO mole ratio at exit vs Inlet temperature

Fig 5.21 shows the variation of H_2/CO mole ratio in the product with temperature at different mole ratio. As the inlet temperature is increased we have seen earlier that the hydrogen production increases however from the above figure it is seen that the H_2/CO mole ratio decreases. This is because water gas shift reaction is mildly exothermic and the reverse reaction is promoted at high temperature increasing the CO formed and decreasing the H_2 .

5.6 Effect of inlet velocity

5.6.1 Effect of inlet velocity on conversion

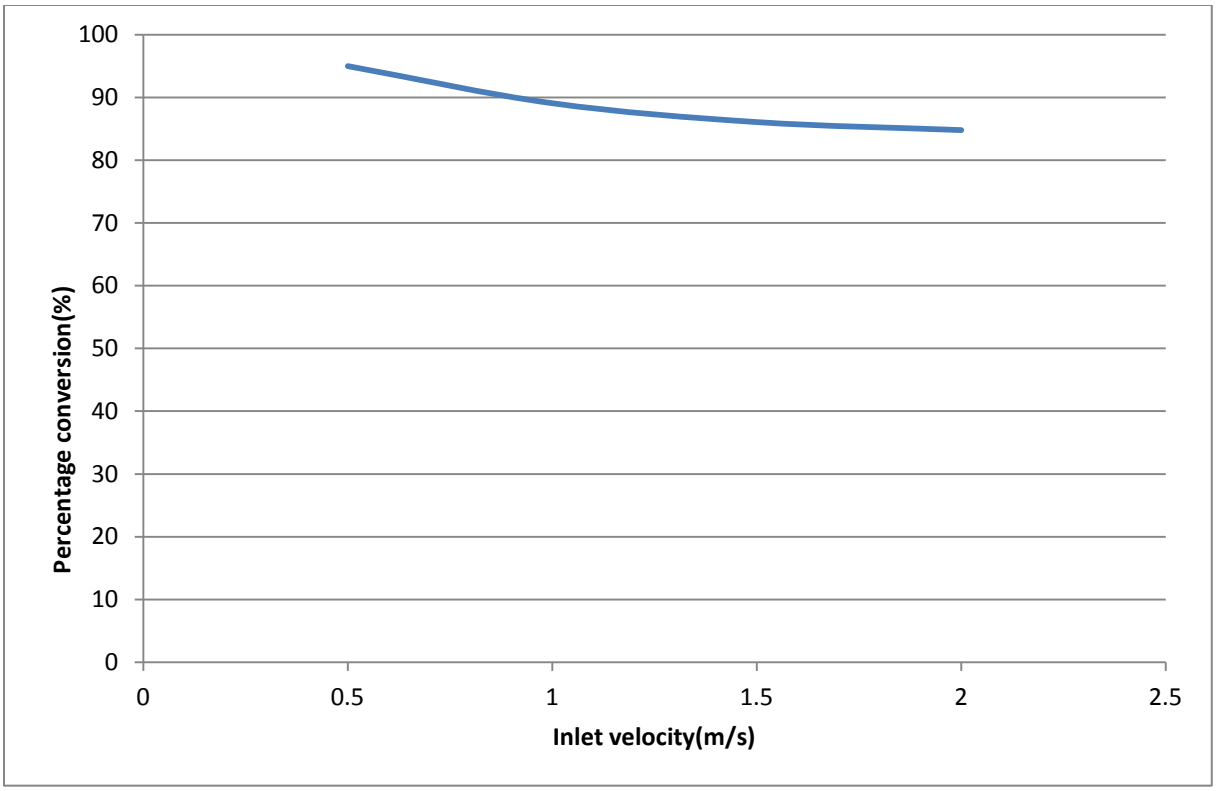

Fig 5.22: Conversion vs inlet velocity (Inlet temp =673K, $CO_2/O_2/CH_4$=1:1:2)

As the inlet velocity is increased from 0.5 m/s to 2m/s the conversion decreases continuously from 94% to 84% at fixed inlet temperature of 673K and fixed inlet composition. This is because the combustion and reforming reactions are assumed to have rates directly proportional to their concentration and increasing the inlet velocity reduces the contact time with the catalyst there by decreasing the conversion of methane.

5.6.2 Effect of inlet velocity on H_2/CO ratio.

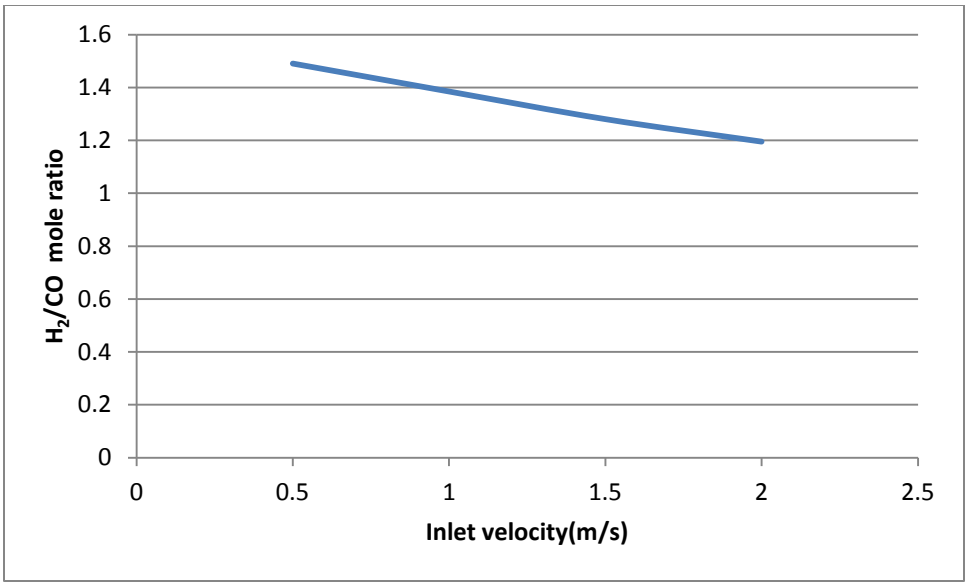

Fig 5.23: Inlet velocity vs hydrogen production (Inlet temp =673K, $CO_2/O_2/CH_4$=1:1:2)

The above figure shows the variation of the H_2/CO mole ratio with the change in space velocity. This is because of the less time available for shift reaction with the increase in the space velocity. The shift reaction occurs only after the combustion and reforming reactions produce CO and H_2O. Due to the increased space velocity to undergo the same amount of completion these reactions take greater length of the reactor. So the time available for the reactant of the shift reaction to react is less. Also from the kinetics we see that the shift reaction is slower as compared to the combustion reaction and reforming reactions under the reaction conditions so increasing the space velocity further reduces the extent of the completion of the reaction. Due to this the amount of hydrogen produced is reduced and the CO does not get converted into CO_2 .

5.7 Effect of O_2 addition

5.7.1 Effect of O_2 addition on methane conversion

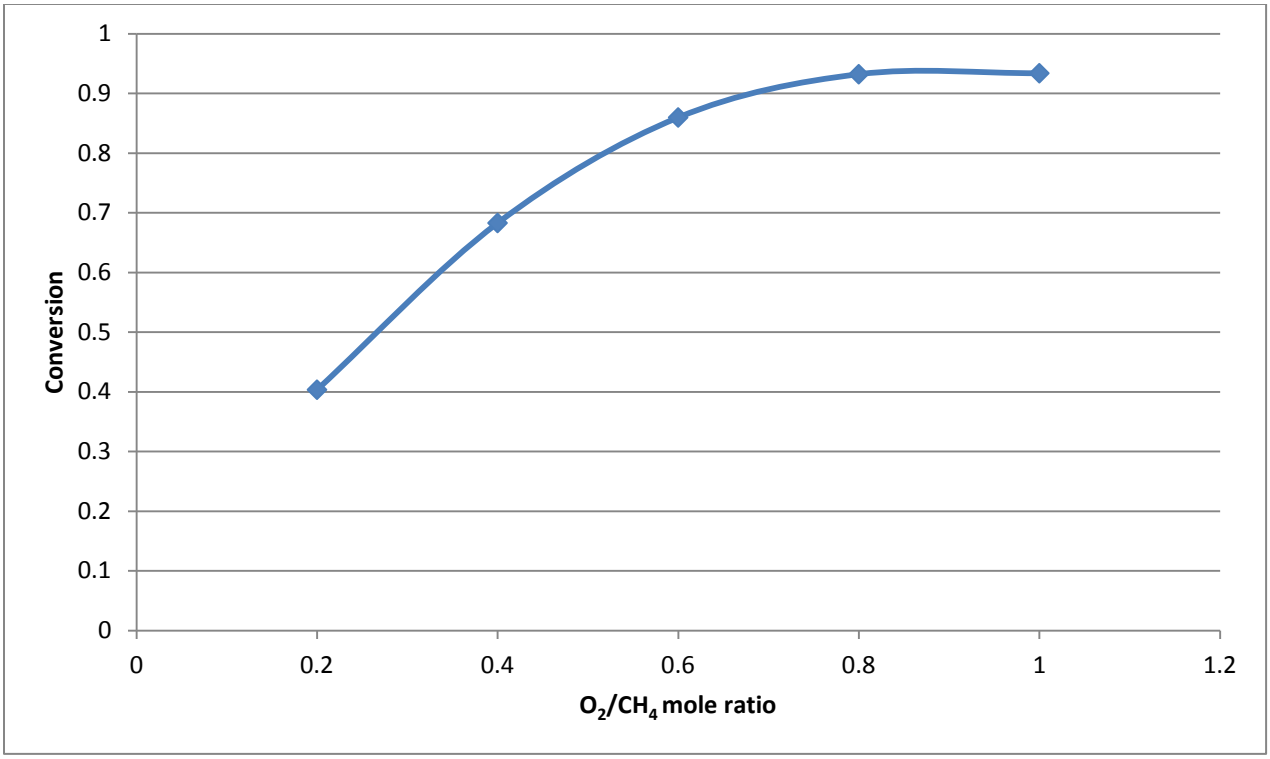

Fig 5.24: CH_4 conversion vs O_2/CH_4 mole ratio(Inlet temperature=673K, CO_2/CH_4 =1)

The above figure shows the variation of CH_4 conversion with the increase in the O_2/CH_4 ratio . The conversion increases from 40% to 93% as the O_2/CH_4 ratio increases from 0.2 to 1 . The increase is primarily because of two reasons . Firstly increase of the oxygen in the feed increases the combustion reaction which increases the conversion. Secondly the increased combustion reaction increases the amount of energy released which increases the endothermic reforming reaction .

5.7.2 Effect of oxygen addition on Hydrogen production

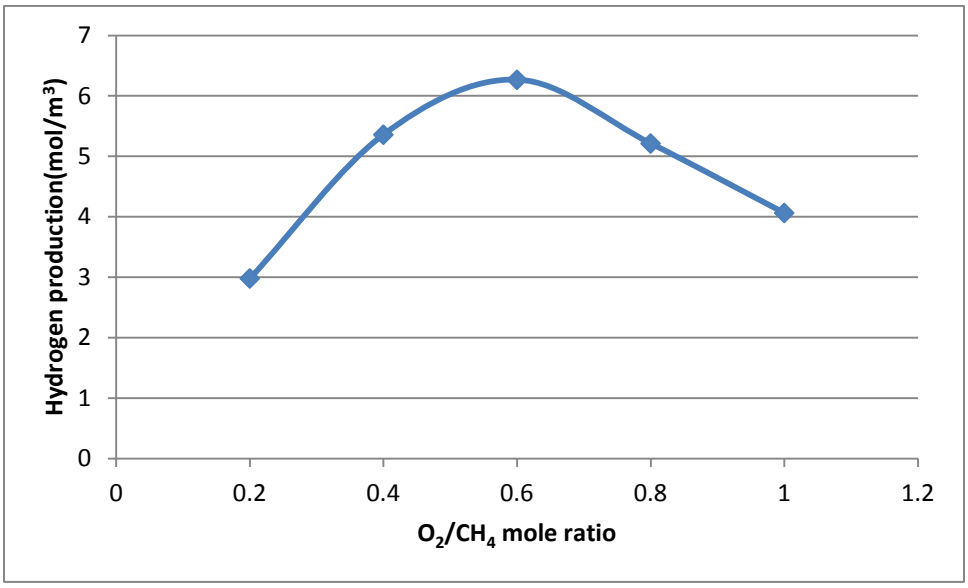

Fig 5.25: Hydrogen production vs O_2/CH_4 mole ratio(Inlet temperature=673K, CO_2/CH_4 =1)

The figure shows the variation of hydrogen production with the increase in the O_2/CH_4 ratio. The hydrogen production increases with the increase in this ratio and reaches to a maximum after that it decreases continuously with the increase in the mole ratio. This is because when the mole ratio is small the combustion reaction does not occur to an appreciable extent and enough energy is not released to drive forward the reforming reaction. With the increase in the oxygen content the reforming reaction is increased due to increased energy availability. But after reaching the optimum value the hydrogen production decreases as most of the methane is consumed in the combustion reactions not in the reforming reactions.

5.7.3 Effect of oxygen addition on H_2/CO ratio

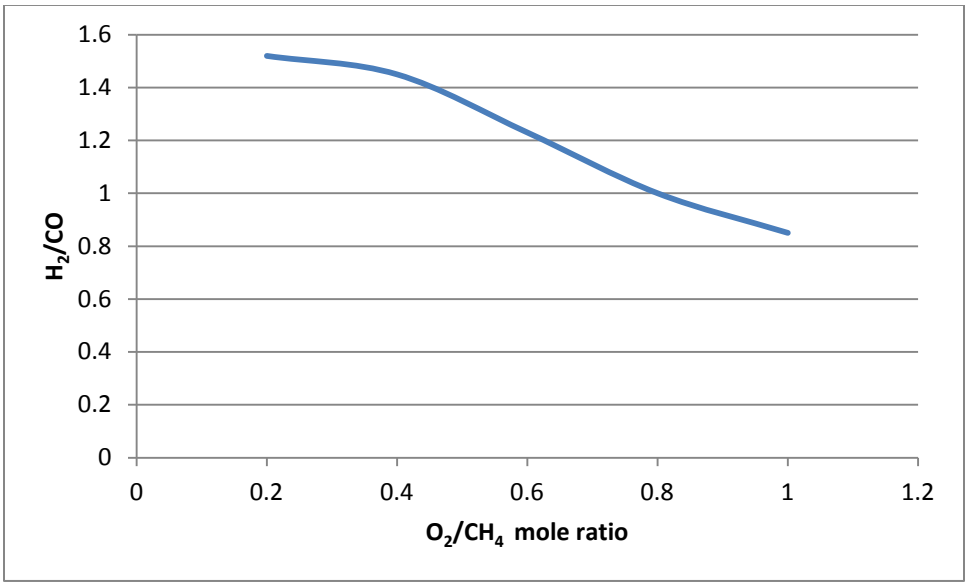

Fig 5.26: H_2/CO vs O_2/CH_4 (Inlet temperature=673K, CO_2/CH_4 =1)

As the O_2/CH_4 ratio is increased from 0.2 to 1.0, the H_2/CO ratio in the product decreases continuously from 1.52 to 0.85 this is because with increased combustion reaction the amount of methane available for reforming reaction decreases . Also since the combustion reaction is exothermic it raise the temperature in the reactor . Due to this reverse water gas shift reaction is promoted which decreases the amount of hydrogen formed and increases the amount of carbon dioxide.

CHAPTER 6

CONCLUSIONS AND RECOMMENDATIONS

In this work oxidative reforming of methane CH_4 in a fluidized bed is modeled and simulated with commercially available CFD software FLUENT 14.5. The Eulerian Eulerian model was used to model the reactor.

The results of the simulation show that

- The addition of CO_2 to the feed along with oxygen increased the hydrogen production and increased the CH_4 conversion.
- The H_2/CO ratio increased with the addition of CO_2 to the feed.
- From the study of the temperature profile it found there is a formation of hot spot along the length of the reactor.
- Increasing the inlet temperature increases the hydrogen production but the corresponding increase in the outlet temperature is not as high.
- Increasing the inlet temperature increases the conversion of methane and there is a decrease in the H_2/CO ratio.
- Increasing the inlet velocity of the reactants reduced the conversion slightly and decreased the H_2/CO ratio.
- The conversion of methane was found to increase with the increase in the oxygen content of the feed.
- The hydrogen production was found to reach a maximum and then decrease with further increase in the oxygen content of the feed.
- The H_2/CO ratio decreased continuously with the increase in the oxygen content.

Recommendations

- Different catalysts such as Pd, Ru can be investigated in the simulation with different rate kinetics for the production of syngas. Pt and Pd are known to stop the formation of hotspots.
- Better results from the simulation studies can be obtained if the Eulerian-Lagrangian model is used instead of the Eulerian-Eulerian model. But the computational requirements increase greatly in case of the Lagrangian model.
- The problem of hot spot can be minimized by the addition of oxygen at different points along the length of the reactor instead of the feed.
- Circulating fast fluidized bed reactors can be used in place of bubbling bed reactors as they are found to give higher conversions.

CHAPTER 7

REFERENCES

[1] Abashar M.E.E.,(2012),' Investigation of hydrogen production in a circulating fast fluidized bed reactor using numerical simulations', Fuel Processing Technology 102 (2012) 73–84.

[2] A´ vila-Neto C.N., Dantas S.C., Silva F.A., Franco T.V.,(2009),'Hydrogen production from methane reforming: Thermodynamic assessment and autothermal reactor design', Journal of Natural Gas Science and Engineering 1 (2009), 205–215.

[3] Barrio V.L., Schaubb G., Rohdeb M,(2007),'Reactor modeling to simulate catalytic partial oxidation and steam reforming of methane. Comparison of temperature profiles and strategies for hot spot minimization', International Journal of Hydrogen Energy 32 (2007), 1421 – 1428.

[4] Benzarti S., Mhiri H., Bournot H.,(2012),'Drag models for Simulation Gas-Solid Flow in the Bubbling Fluidized Bed of FCC Particles', World Academy of Science, Engineering and Technology 61 2012.

[5] Corbo Pasquale, Migliardini Fortunato,(2007), 'Hydrogen production by catalytic partial oxidation of methane and propane on Ni and Pt catalysts 'International Journal of Hydrogen Energy 32 (2007), 55 – 66.

[6] Dantas S.C., Resende K.A., Rossi R.L., Assis A.J., (2012),'Hydrogen production from oxidative reforming of methane on supported nickel catalysts: An experimental and modeling study', Chemical Engineering Journal 197 (2012), 407–413.

[7]De Groote Ann M, Froment Gilbert F.,(1995),'Simulation of the catalytic partial oxidation of methane to synthesis gas', Applied Catalysis A: General 138 (1996), 245-264.

[8] Dou Binlin, Song Yongchen,(2010),'A CFD approach on simulation of hydrogen production from steam reforming of glycerol in a fluidized bed reactor', International Journal Of Hydrogen Energy 35(2010), 781-790.

[9] Fluent ,Inc. FLUENT 6.3 user's guide. Lebanon, NH:FLuent Inc. 2006.

[10] Freitas Antonio C. D., Guirardello Reginaldo,(2012),'Oxidative reforming of methane for hydrogen and synthesis gas production: Thermodynamic equilibrium analysis ', Journal of Natural Gas Chemistry 21(2012), 571–580.

[11] Hou Kaihu, Hughes Ronald,(2001),'The kinetics of methane steam reforming over a Ni/a-Al_2O catalyst' Chemical Engineering Journal 82 (2001),311–328.

[12] Jing Q.S, Fei J.H., Lou H, (2007),'Effective reforming of methane with CO_2 and O_2 to low H2/CO ratio syngas over Ni/MgO–SiO_2 using fluidized bed reactor', Energy Conversion and Management 45 (2004),3127–3137.

[13] Li Yunhua, Wang Yaquan, Zhang Xiangwen, Mi Zhentao,(2008),'Thermodynamic analysis of autothermal steam and CO_2 reforming of methane', International Journal Of Hydrogen Energy 38(2005), 2507-2514.

[14] Moreno L. Pe´rez, Soler J., Herguido J, (2013),'Stable hydrogen production by methane steam reforming in a two-zone fluidized-bed reactor: Effect of the operating variables', International Journal Of Hydrogen Energy 45(2013), 7830-7838.

[15] Park Nonam, Park Myung-June, Baek Seung-Chan, (2014),'Modeling and optimization of the mixed reforming of methane: Maximizing CO_2 utilization for non-equilibrated reaction', Fuel 115 (2014), 357–365.

[16] Rowshanzamir S. , Safdarnejada S. M., Eikanib M. H.,(2012),'A CFD model for methane autothermal reforming on Ru/ Al_2O_3 catalyst', Procedia Engineering 42 (2012),2 – 24.

[17] Taghipour Fariborz, Ellis Naoko, Wong Clayton,(2005),'Experimental and computational study of gas–solid fluidized bed hydrodynamics', Chemical Engineering Science 60 (2005), 6857 – 6867.

[18] Srivastava Vimal Chandra,(2014),' Simulation of fluidized bed reactor for producing synthesis gas by catalytic CH_4–CO_2 reforming', Journal of CO_2 Utilization 5 (2014),10–16.

[19] Xuli Zhai a, Shi Ding, Zhihong Liu , Yong Jin , Yi Cheng,(2011)'Catalytic performance of Ni catalysts for steam reforming of methane at high space velocity', International Journal Of Hydrogen Energy 41(2011), 482-489.

[20] Yin Lijie , Wang Shuyan, Lua Huilin, Ding Jianmian,(2007),'Simulation of effect of catalyst particle cluster on dry methane reforming in circulating fluidized beds ',Chemical Engineering Journal 131 (2007),123–134.